Reviews

Inorganic Materials as Catalysts for Photochemical Splitting of Water

Frank E. Osterloh*

Department of Chemistry, University of California, Davis, One Shields Avenue, Davis, California 95161

Received August 25, 2007. Revised Manuscript Received October 18, 2007

Photochemical splitting of water into H_2 and O_2 using solar energy is a process of great economic and environmental interest. Since the discovery of the first water splitting system based on TiO_2 and Pt in 1972 by Fujishima and Honda, over 130 inorganic materials have been discovered as catalysts for this reaction. This review discusses the known inorganic catalysts with a focus on structure–activity relationships.

Introduction

At a power level of 1000 W/m,[2] the solar energy incident on the earth's surface by far exceeds all human energy needs.[1,2] Photovoltaic[3] and electrochemical solar cells[3–5] that convert solar energy into electricity can reach up to 55–77% efficiency[6–8] but remain uneconomical because of high fabrication costs, insufficient light absorption,[9] and inefficient charge transfer.[3] In a process that mimics photosynthesis, solar energy can also be used to convert water into H_2 and O_2, the fuels of a H_2-based energy economy.

$$H_2O \rightarrow \tfrac{1}{2}O_2(\Delta) + H_2(g); \quad \Delta G = +237\ \text{kJ/mol} \quad (1.3\ \text{eV/e}, \lambda\text{min} = 1100\ \text{nm}) \quad (1)$$

Reaction 1 is catalyzed by many inorganic semiconductors, the first of which, TiO_2, was discovered in 1971 by Fujishima and Honda (see below).[10,11] Today, over 130 materials and derivatives are known to either catalyze the overall splitting of water according to eq 1 or cause water oxidation or reduction in the presence of external redox agents. Current record holders in terms of quantum efficiencies (QEs) are NiO-modified La/$KTaO_3$ (QE = 56%, pure water, UV light),[12] ZnS (QE = 90%, aqueous Na_2S/Na_2SO_3, light with $\lambda > 300$ nm),[13] and Cr/Rh-modified GaN/ZnO (QE = 2.5%, pure water, visible light).[14,15] So far, no material capable of catalyzing reaction 1 with visible light and a QE larger than 10% has been found. Here, 10% is the limit for commercial applications.[16] In order to highlight recent developments and to identify promising directions in this increasingly complex research area, this review summarizes the known inorganic catalysts and discusses property−activity relationships with a focus on structural features. After a brief introduction of the basic physical concepts, catalysts are presented starting with the transition element oxides, followed by the main-group element oxides, nitrides, and phosphides, and the sulfides. The review concludes with a brief discussion of important criteria for effective catalysts. Readers interested in other aspects of solar-energy utilization and photocatalysis are referred to a series of excellent review articles on renewable energy,[1,17,18] general photocatalysis,[19–21] water oxidation catalysts,[22,23] photosystem II,[24] molecular,[25,26] colloidal,[27–32] and heterogeneous water splitting catalysts,[33–46] including transition-metal oxides,[38–43,47–49] metal oxynitrides,[44–46] and photoelectrochemical cells and their physical principles.[8,16,18,50–61]

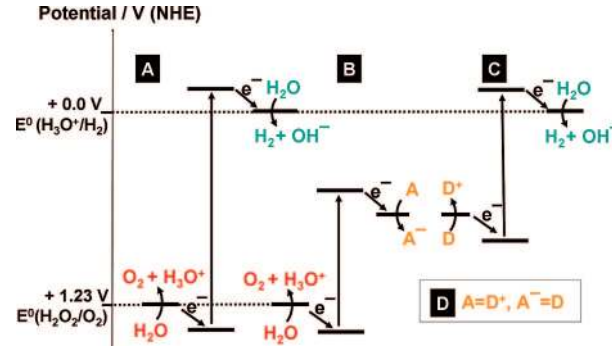

Figure 1. Potential energy diagrams for photochemical water splitting at pH = 0: (A) single semiconductor system; (B) with an electron acceptor; (C) with an electron donor; (D) dual semiconductor system (z scheme) employing a redox shuttle. Modified from ref 108.

General Principles

The photocatalytic properties of inorganic semiconductors strongly depend on the electronic band structure. For photochemical water reduction to occur, the flat-band potential of the semiconductor (for highly doped semiconductors, this equals the bottom of the conductance band) must exceed the proton reduction potential of 0.0 V vs NHE at pH = 0 (−0.41 V at pH = 7; Figure 1A). To facilitate water oxidation, the potential of the valence band edge must exceed the oxidation potential of water of +1.23 V vs NHE at pH

* E-mail: fosterloh@ucdavis.edu.

10.1021/cm7024203 CCC: $40.75
Published on Web 12/11/2007

= 0 (+0.82 V at pH = 7). Based on these parameters, a theoretical semiconductor band-gap energy of ~1.23 eV is required to drive the water-splitting reaction according to eq 1. The smallest band gap achieved so far in a functional catalyst is 2.30 eV in NiO/RuO_2−Ni:$InTaO_4$.[47,62] Semiconductors with smaller band gaps or lower flat-band potentials require a bias voltage or external redox reagents to drive the reaction (Figure 1B/C). Alternatively, two or more small-band-gap semiconductors can be combined to drive water oxidation/reduction processes separately via multiphoton processes (Figure 1D).

Surprisingly, literature values for flat-band potentials[35,50,55,63–68] exhibit large variations; e.g., reported values for Ta_2O_5 range from −0.3[69] to −1.4 V.[64] Discrepancies reflect experimental uncertainties[69] and intrinsic differences resulting from variable material preparations. It is well-known that flat-band potentials strongly depend on ion absorption (protonation of surface hydroxyl groups), crystallographic orientation of the exposed surface, surface defects, and surface oxidation processes (sulfur on CdS).[70,71] These and other factors[55,72] are rarely considered in the preparation and testing of photochemical water-splitting catalysts. For the design of new materials, it can therefore be useful to estimate the flat-band potentials with a method developed by Butler and Ginley.[73] If the geometric mean χ of the Mulliken electronegativities of the semiconductor constituents is known, the flat-band potential V_{fb} [V vs NHE] for a *metal oxide* can be calculated as

$$V_{fb} = E_0 - \chi + \tfrac{1}{2}E_G \qquad (2)$$

Here E_G is the semiconductor band gap [eV] and E_0 (+4.44 eV) is the energy of a free electron on the H_2 redox scale.[60,73,74] Activities of photochemical water-splitting catalysts are usually assessed with the rates of evolved gases [mol/h] per catalyst amount [g] under the specified irradiation conditions. From the measured evolution rate [H_2], the apparent QE = 2[H_2]/I of the catalyst can be calculated using the known photon flux I [mol/s] incident on the reaction mixture (as determined by, e.g., ferrioxalate actinometry[75]). If available, this information is included with the experimental conditions in Table 1. The structures of selected semiconductors are shown in Figures 2−4.

TiO_2

The photocatalytic properties of TiO_2 have been reviewed previously.[16,27,29,32,33,76–78] Titania (TiO_2) was the first material described as a photochemical water-splitting catalyst. It crystallizes in three structure types: Rutile, Anatase, and Brookite. All modifications contain TiO_6 octahedra that are interconnected via two (Rutile), three (Brookite), or four (Anatase) common edges and via shared corners, and as a result, the band gaps (3.0 eV for Rutile and 3.15 eV for Anatase) differ slightly.[67] In their 1971/72 papers, Fujishima and Honda described an electrochemical cell consisting of a n-type TiO_2 (Rutile) anode and a Pt black cathode.[10,11] When the cell was irradiated with UV light (<415 nm) from a 500 W Xe lamp, O_2 evolution takes place at the anode and a current flows to the Pt counter electrode. Based on the current, a photoelectrochemical efficiency of ~10% was estimated. While formation of H_2 at the cathode was not confirmed in the original paper, Wrighton et al. showed in 1975 that O_2 and H_2 were indeed formed under similar conditions and that they were both from water.[79] In the same year, the first report of photocatalytic water splitting by a powdered TiO_2 catalyst appeared.[80] When wetted TiO_2 powder (Table 1) was exposed to water vapor under UV/vis irradiation, H_2 and O_2 were evolved at a near stoichiometric ratio. In the presence of N_2, NH_3 was produced, while HCCH gave CH_4, C_2H_4, and C_2H_6. Thermal annealing and storage conditions greatly affected the activity of the catalyst, which was most active as a mixture of 23% Rutile and 77% Anatase. These findings were disputed by Van Damme and Hall,[81] who attributed the observed reactivity to photolytic decomposition of hydroxyl groups on the TiO_2 surface, as opposed to a catalytic process. However, Kawai and Sakata demonstrated only 1 year later that catalytic amounts of D_2 were produced when a heat-treated TiO_2 powder was irradiated in the presence of D_2O vapor.[82] No O_2 was evolved when pure Rutile was used, but the addition of RuO_2 led to a functional catalyst that produced both D_2 and O_2 after the initial formation of CO as a side product.

In the late 1970s, titania catalysts were improved significantly following ideas that were first expressed by Nozik.[55,83] In his 1977 paper, Nozik proposed the concept of "photochemical diodes" (later termed antenna catalysts[84]), which consisted of two electrodes from a photoelectrochemical cell directly fused together. This produced either p−n-type (e.g., p-GaP/n-TiO_2) or Schottky-type devices (e.g., n-CdS/Pt or p-GaP/Pt). The efficiency of such dual-component catalysts was expected to improve because a space charge layer at the material interface enhances electron–hole separation. Accordingly, in 1980, Sato and White found that enhanced evolution of H_2/O_2 took place on a TiO_2 catalyst to which a Pt cocatalyst had been added via photodecomposition of hexachloroplatinate in an acetic acid solution.[85] In this study, ^{18}O-labeling experiments also confirmed O_2 production from water. Without Pt, no H_2 was formed on Anatase TiO_2. However, as a drawback, the Pt portion in the material catalyzed the reverse of the water-splitting reaction according to eq 1, limiting yields at high H_2 partial pressure. Following earlier work on molecular dyes,[86–88] Graetzel's group published a series of papers in the 1980s on multicomponent catalysts comprised of colloidal TiO_2 (Anatase) particles doped with 0.4% of Nb_2O_5 and joined together with Pt metal and with RuO_2 particles.[29,89–92] Under UV irradiation, aqueous suspensions of these particles produced stoichiometric amounts of H_2 and O_2. Here, TiO_2 generates the electron−hole pair, of which the electron is subsequently transferred to the Pt water reduction site and the hole to the RuO_2 water oxidation site.[92] Again, slow recombination of H_2 and O_2 took place in the dark because of the Pt cocatalyst. By the addition of $[Ru(bpy)_3]^{2+}$ as a sensitizer,[92] the system was able to split water under visible light irradiation. Here, the electron–hole pair is generated on the $[Ru(bipy)_3]^{2+}$ complex, and the role of the TiO_2 particle is merely to accept the electron from the sensitizer and to funnel it to Pt, where H_2 evolution occurs. The sensitizer is subsequently reduced at the RuO_2 site, which oxidizes water to O_2. The overall

Table 1. Catalyst Overview

no.	material	cocatalyst	irradiation conditions	reaction details and refs
1a	TiO_2		UV, 360 W Hg	H_2/O_2 at 1.16/0.55 μmol/h/0.2 g of cat[80]
1b	TiO_2	Pt	UV, 200 W Hg	H_2 and O_2 in stoich. ratio (0.1 μmol/h of H_2 per 250 mg of cat.. [85]
1c	Nb_2O_5:TiO_2 (Anatase)	Pt and RuO_2	450 W Xe at >400 nm	up to 5 mL/h/0.1 g of H_2 (222 μmol/h/0.1 g) from aqueous EDTA and up to 4.5 mL/h/0.05 g of H_2 (200 μmol/h/0.1 g) from water with stoich. O_2;[89] See also refs 29, 90, and 92; for Pt/RuO_2/TiO_2, QE up to 30% under UV[91] and up to 5% with $[Ru(bpy)_3]^{2+}$ sensitizer under vis light[92]
1d	TiO_2	Pt	200 W Hg at 440 nm	3–4 mL of H_2 after 5 h; pH = 4.78 using $Ru(bipy)_3]^{2+}$, MV^{2+}, as an electron relay and EDTA as a sacrif. donor; cat. < 1 mg[84]
1e	TiO_2	Pd and Rh	UV, 500 W Xe	449 μmol/h/0.3 g (QE = 29%) for Rh/TiO_2 compared to 284 μmol/h/0.3 g (QE = 17%) for Pt/TiO_2[95]
1f	TiO_2 Anatase and Rutile	Pt	UV at >300 nm, 400 W Hg	H_2 (180 μmol/h/0.5 g) and O_2 (90 μmol/h/0.5 g) from water at pH = 11 (QE = 4%)[107,108]
1g	N-doped TiO_2	Pt	450 W Xe at >420 nm	21 μmol/h/g (QE = 14%) of O_2, traces of H_2; $AgNO_3$ as the acceptor[113]
2a	$SrTiO_3$	NiO	450 W Hg	stoich. water *vapor* splitting at 4.4×10^{-3} mL/h/2.0 g (H_2);[116] different study, 100 μmol of H_2/h/g with stoich. O_2[117]
2b	Cr/Ta:$SrTiO_3$	Pt	300 W Xe at 420.7 nm	splits water into H_2/O_2 at 0.21/0.11 μmol/h in tandem with Pt−WO_3 (0.4 g of both cat., QE = 0.1%);[118] Cr/Ta:$SrTiO_3$-Pt produced H_2 at 0.8 μmol/h/0.2 g from KI(aq); Pt−WO_3 alone with $NaIO_3$ produced O_2 at 84 μmol/h/0.2 g
2c	$SrTiO_3$	Ru, Ir, Pd, Pt, Os, Re, Co	1000 W Xe/Hg at >300 nm	stoich. amounts of H_2/O_2 from pure water; all values for 0.05 g of cat. are Rh/$SrTiO_3$ = 628 μmol L/h, Ru/$SrTiO_3$ = 159 μ L/h, Re = 107 μmol L/h, Ir = 80 μ L/h, Pt = 107 μmol L/h, Pd = 71 μ L/h, Os = 62 μmol L/h, Co = 26 μ L/h, $SrTiO_3$ = 11 μmol L/h of H_2 but no O_2[119,120]
3, **4**	La_2TiO_5, $La_2Ti_3O_9$	NiO	UV at 450 W Hg	H_2/O_2 in stoich. ratio at 386 μmol/h/g ($La_2Ti_3O_9$) and 442 μmol/h/g (La_2TiO_5)[121]
5a	$La_2Ti_2O_7$	NiO	UV at 450 W Hg	307 and 152 μmol/h/0.5 g of H_2/O_2;[123] another study reports 441 μmol/h/g of H_2 with stoich. O_2 (QE = 12%);[122] doping with BaO and addition of NaOH gives 5 mmol of H_2/h/g with stoich. O_2;[121] H_2 at rates of 120 (Pt cocat.) and 400 μmol/h/g (NiO, O_2 not measured);[124] hydrothermal synthesis: 72.5 μmol of H_2/h/g (500 W Hg, O_2 not determined)[125]
5b	$La_2Ti_2O_7$, doped with Fe, Cr	Pt	500 W Hg at >420nm	H_2 at <15 μmol/h/g from MeOH(aq)[124]
6	$Sr_3Ti_2O_7$		UV, 400 W Hg	~20 μmol/h/g of H_2; with NiO; 77 μmol/h/g with stoich. O_2; rate increase for NiO-modified material from ester pyrolysis 144 μmol/h/g with stoich. O_2 evol.[126]
7	$PbTiO_3$	Pt	450 W Xe at >420 nm	13.6/523 μmol/h/0.3 g of H_2/O_2 from aqueous MeOH and $AgNO_3$[127]
8	$Sm_2Ti_2S_2O_5$	Pt	300 W Xe at 440–650 nm	38 μmol/h/0.2 g (QE = 0.1%) of H_2 with Na_2S−Na_2SO_3 or methanol; $Sm_2Ti_2S_2O_5$−IrO_2 gives O_2 at 11 μmol/h/0.2 g (QE = 1.1%) from aqueous $AgNO_3$[128]
9–11	$M_2La_2Ti_3O_{10}$ (M = K, Rb, Cs), doped with Nb	Pt	UV, 450 W Hg	stoich. H_2/O_2 of 79 μmol/h/g (for $Rb_2La_2Ti_2NbO_{10}$) to 869 μmol/h/g (for $Rb_2La_2Ti_3O_{10}$, QE = 5%);[129–131] activity of $K_2La_2Ti_3O_{10}$ depends on the cocat. (Ni, Pt, or RuO_2) and on the KOH conc.[133] different synthesis gives 2.89 mmol of H_2/h/g and 1.13 mmol of O_2/h/g;[134] Au-modified $K_2La_2Ti_3O_{10}$ gave H_2 at 841 μmol/h/g from a 0.1 M KOH solution; O_2 not meas.[132]
12	$PbBi_4Ti_4O_{15}$	Pt	450 W Xe at >420 nm	11.2/433 μmol/h/0.3g of H_2/O_2 employing MeOH and $AgNO_3$ as sacrif. agents.[127]
13	$BaTi_4O_9$	RuO_2	UV, 400 W Xe	H_2 at 180 μmol/h/g with stoich. O_2[42,259]
14–16	$M_2Ti_6O_{13}$ (M = Na, K, Rb)	RuO_2	UV, 400 W Xe	H_2/O_2 rates highest for M = Na (17/8 μmol/h/g)[42,135]
17	$La_4CaTi_5O_{17}$	NiO	450 W Hg at >320 nm	499 μmol/h/g of H_2 and stoich. O_2 (QE = 20%)[122]
18	$M_3(PO_4)_4$ (M = Ti, Zr)	Pt	300 W Xe at >290 nm	Pt/$Ti_3(PO_4)_4$ (0.91 μmol/h/g), Pt/$M_3(PO_4)_4$ (M = 50% Ti, 50% Zr, 5.91 μmol/h/g)[136]
19	Ta_2O_5	NiO_x, Pt, or RuO_2	UV, 400 W Hg	190 μmol/h/g with stoich. O_2 yield[40] and 1150/530 μmol/h/g under optimized conditions[48]
20, **21**	$A_4Ta_xNb_{6-x}O_{17}$ (A = Rb, K, x = 1−4)	NiO	400 W Hg	100−936 μmol of H_2/h/g of cat. (stoich. O_2 evol.); activity decreases with increasing Ta content[140]
22–24a	$MTaO_3$ (M = Li, Na, K)	NiO	UV, 400 W Hg	H_2 and O_2 from pure water at 3.39 and 1.58 mmol/h/g (QE = 20–28%, at 270 nm);[48,141,142] 10–40 times lower activity without cocat.;[142] sol–gel method produces active cat. with H_2/O_2 1940/~1000 μmol/h/g[143]

Table 1. Continued

no.	material	cocatalyst	irradiation conditions	reaction details and refs
24b	La:$NaTaO_3$	NiO	UV, 400 W Hg	H_2 and O_2 at 19.8 and 9.7 mmol/h/g, from pure water[12] (QE = 56%)
25	$La_{1/3}TaO_3$	NiO	UV, 400 W Hg	35/7.9 μmol/h/0.5 g of H_2/O_2 from water[144]
24c	$KTaO_3$ doped with Ti, Zr, Hf	NiO	500 W Xe	H_2/O_2 from pure water at rates of up to 100/30 μmol/h/0.1 g;[145] Ti works best (at 8% doping level), followed by Zr and Hf
24d	Zr:$NaTaO_3$	Pt	UV, 500 W Xe	Zn, Co, Cr, and Mg porphyrin as the sensitizer; up to 57/28 μmol/h/0.1 g of H_2/O_2 from pure water (for cyanocobalamin); QE up to 12.8%[146]
26a/b	Ni:$InTaO_4$, $InTaO_4$	RuO_2 or NiO	400 W Hg and 300 W Xe at >420 nm	H_2/O_2 from pure water at rates of 16.6/8.3 μmol/h/0.5 g with QE = 0.66%; nondoped NiO−$InTaO_4$ gave 3.2/1.1 μmol/h[47,62]
27–29	MTa_2O_6 (M = Sr, Ba, Sn)	NiO, Pt	UV, 400 W Hg	NiO−$SrTa_2O_6$ gives H_2/O_2 from pure water at up to 960/490 μmol/h/g (QE = 7%);[147–149] $BaTa_2O_6$ (orthorhombic) gives 33/15 μmol/h/g and 780/350 μmol/h/g with $Ba(OH)_2$ and NiO cocat.;[48] Pt/$SnTa_2O_6$ makes 2.1 μmol/h/0.3 g of H_2 under UV from MeOH(aq)[179]
30–34	MTa_2O_6 (M = Ni, Mn, Co) and $MTaO_4$ (M = Cr, Fe)		UV, 400 W Hg	M = Ni gave H_2/O_2 at 11/4 μmol/h/g, M = Mn, Co, and $CrTaO_4$, $FeTaO_4$ gave only traces of H_2[48]
35	$Ca_2Ta_2O_7$	NiO	450 W Hg	170/83 μmol of H_2/O_2 per 0.5 g from pure water[148]
36, 37	Bi_2MTaO_7 (M = La, Y)		400 W Hg	Bi_2LaTaO_7 was slightly more active with H_2/O_2 at 41.8/20.5 μmol/h/g from pure water[150]
38	$Sr_2Ta_2O_7$	NiO	UV, 400 W Hg	H_2/O_2 from pure water at 2141/1059 μmol/h/0.5 g[149,151]
39–41	$M_2La_{2/3}Ta_2O_7$ (M = K, H), $H_2SrTa_2O_7$	NiO	UV, 400 W Hg	H_2/O_2 from pure water at rates of 262/− ($K_2La_{2/3}Ta_2O_7$), 940/459 ($H_2La_{2/3}Ta_2O_7$), 240/59 μmol/h/0.5 g ($H_2SrTa_2O_7$); without NiO. the rates are half, except for $H_2SrTa_2O_7$, which is more active (385/179 μmol/h/0.5 g)[144]
42	$K_2Sr_{1.5}Ta_3O_{10}$	RuO_2	400 W Hg	H_2/O_2 from pure water at 100/39.4 μmol/h/0.5 g (QE = 2%); without cocat. activity reduced to 17% of these values[152]
43	$KBa_2Ta_3O_{10}$	NiO	400 W Hg	150 μmol/h/g of H_2 (QE = 8%)[122]
44–46	$Sr_4Ta_2O_9$, $M_5Ta_4O_{15}$ (M = Sr, Ba)	NiO	400 W Hg	H_2/O_2 from pure water at 32/2 μmol/h/0.5 g ($Sr_4Ta_2O_9$) and 1194/722 μmol/h/0.5 g ($Sr_5Ta_4O_{15}$);[149] $Ba_5Ta_4O_{15}$ gave up to 2.08/0.91 mmol/h/g of H_2/O_2 and 7.1/3.6 mmol/h/g in the presence of $Ba_{0.5}TaO_3$ traces[153]
47	$K_3Ta_3Si_2O_{13}$	NiO	UV, 400 W Hg	H_2/O_2 at 43/19 μmol/h/g; NiO improves activity to 368/188 μmol/h/g[154]
48	$K_3Ta_3B_2O_{12}$		450 W Hg	0.5 g of cat. produced 2.4/1.2 mmol of H_2/O_2 per h from pure water; addition of NiO did not improve the activity[155]
49–52	R_3TaO_7 (R = Y, Yb, Gd, La)		400 W Hg	La_3TaO_7 (Weberite), 164/82 μmol/h/0.5 g of H_2/O_2 from pure water; Pyrochlore, 4/1 μmol/h/0.5 g;[123,156] for R = Y, Yb, only H_2 traces
53–57	$LnTaO_4$ (Ln = La, Ce, Pr, Nd, and Sm)	NiO	400 W Hg	only NiO-modified $LaTaO_4$ has signif. cat. activity with H_2/O_2 at rates of 115.6/51.5 μmol/h/0.2 g[157]
58–61	$RbLnTa_2O_7$ (Ln = La, Pr, Nd, and Sm)		UV, 400 W Hg	up to 47/25.3 μmol/h/0.2 g of H_2/O_2 ($RbNdTa_2O_7$) from pure water; NiO cocat., 117.2/58.7 μmol/h/0.2 g; non-NiO-modified $NaNdTa_2O_7$, 2.4/<0.1 μmol/h/0.2 g[158,159]
62, 63a	$M_4Nb_6O_{17}$ (M = K, Rb)		UV, 450 W Hg	M = K gives nonstoich. water splitting at a low rate;[160] addition of NiO gives H_2/O_2 at rates of 70/35 μmol/h/g; under opt. conditions, QE = 5.3–20%;[122,161–163] after internal platinization with $[Pt(NH_4)_4]^{2+}$, 45 μmol/h/g of H_2 with stoich. O_2, QE = 1.3%;[164] for M = Rb, QE = 10% was observed with NiO[43]
63b	$K_4Nb_6O_{17}$−TiO_2 intercalated		UV, 450 W Hg	1 g of this material in pure water at 60 °C evolved 1 mL of gases per h; H_2/O_2 content was not determined[165]
63c	$K_4Nb_6O_{17}$, H^+-exchanged	Pt	500 W Hg/Xe at >400 nm	0.2 μmol/h/0.1 g of H_2 for $K_2H_2Nb_6O_{17}$ (QE = 0.3%) from aqueous HI in the presence of $[Ru(bpy)_3]^{2+}$ sensitizer[74,168]
64–66	KNb_3O_8, $KTiNbO_5$, $CsTi_2NbO_7$	Pt	500 W Hg/Xe at >400 nm,	<0.2 μmol/h/0.1 g of H_2 from aqueous HI with $[Ru(bpy)_3]^{2+}$ sensitizer[74,168]
67a−d	$A[M_{n-1}Nb_nO_{3n+1}]$ (A = H, K, Rb, Cs; M = Ca, Sr, Na, Pb; n = 2–4)	Pt	UV, 450 W Hg	Pt-mod. cat. produces up to 100 μmol/h/g of H_2 but no O_2 (value for $KCa_2Nb_3O_{10}$) from MeOH(aq); $HCa_2Nb_3O_{10}$ gives 5.9 mmol/h/g; modified with Pt increases the rate to 19 mmol/h/g;[38,43,169] 620 μmol/h/0.1 g for restacked Pt/$HCa_2Nb_3O_{10}$ from MeOH(aq) (500 W Xe lamp);[172] 8.1 mmol/h/g of H_2 for Pt/$HCa_2Nb_3O_{10}$/SiO_2 from MeOH(aq)[171]
67b	$KCa_2Nb_3O_{10}$	RuO_2	450 W Hg	H_2 at 3.8 μmol/h/0.3 g from pure water but no O_2; intercalation with RuOx gives H_2/O_2 at 96/47 μmol/h/0.3 g[170]

Table 1. Continued

no.	material	cocatalyst	irradiation conditions	reaction details and refs
67c	$HCa_2Nb_3O_{10}$	Pt	750 W Hg	individual nanosheets produce H_2 at 2.28 μmol/h/0.1 g from pure water (QE = 0.22%) and 78 μmol/h/0.1 g after modification with Pt (QE = 7.5%); no O_2 is produced[173]
68	$K_{0.5}La_{0.25}Bi_{0.25}Ca_{0.75}Pb_{0.75}Nb_3O_{10}$	Pt	450 W Xe at >420 nm	traces of H_2 and 168 μmol/h/0.3 g of O_2 from MeOH(aq)/$AgNO_3$[127]
69, **70**	$MPb_2Nb_3O_{10}$ (M = Rb, H)	Pt	500 W Xe at >420 nm	cat. with M = Rb evolves H_2 traces from MeOH(aq); Pt-modified $HPb_2Nb_3O_{10}$ gives ~4 μmol/h/g and internally platinized cat. gives ~14.5 μmol/h/g from MeOH(aq)[174]
71	$PbBi_2Nb_2O_9$	Pt	450 W Xe at >420 nm	7.6 μmol/h/g of H_2 (QE = 0.95%) from MeOH(aq); using $AgNO_3$, it produces O_2 at a rate of 520 μmol/h/g (QE = 29%)[113]
72	Bi_3TiNbO_9	Pt	UV, 450 W Hg	33 μmol/h/g of H_2 from MeOH(aq) and 31 μmol/h/g of O_2 from aqueous $AgNO_3$[175]
73–77	Bi_2MNbO_7 (M = Al, Ga, In), M_2BiNbO_7 (M = Ga, In)		UV, 400 W Hg	Bi_2MNbO_7 from H_2 from MeOH(aq) and O_2 from $Ce(SO_4)_2$ solution at rates up to 710 and 25 μmol/h/g, respectively; cat. with M = Al was most active;[47] M_2BiNbO_7 evolve 54.3 (In) and 72.6 (Ga) μmol/h/g of H_2 with stoich. O_2[177]
78	$ZnNb_2O_6$		UV, 400/450 W Hg	small amounts of H_2 but no O_2; with NiO water splitting with 54/21 μmol/h/g of H_2/O_2[151,178]
79	$SnNb_2O_6$	Pt	300 W Xe at >420 nm	evolves H_2 at 18 μmol/h/0.3 g from MeOH(aq) solution with a Pt cocat.[179]
80	$Sr_2Nb_2O_7$		UV, 450 W Hg	NiO-loaded $Sr_2Nb_2O_7$ produced H_2/O_2, at rates of 110/36 μmol/h/g; without NiO, only H_2 was produced;[151] larger activity (402/198 μmol/h/g of H_2/O_2 and QE = 23%) were observed by Lee and co-workers[122]
81	$Ca_2Nb_2O_7$	NiO	UV, 450 W Hg	H_2 at a rate of 101 μmol/h/g with a QE = 7%;[122] O_2 not determined
82	$Ca_2Nb_4O_{11}$		UV, 400 W Hg	1.7/0.8 mmol/h/0.5 g of cat.[180]
83	$Ba_5Nb_4O_{15}$	NiO	400 W Hg	from pure water H_2 and O_2 are evolved at 650/250 μmol/h/0.5 g (solid-state reaction) and 2366/1139 μmol/h/0.5 g (preparation from metal citrates)[181]
84	$BiVO_4$		300 W Xe at >520 nm	O_2 at 31 μmol/h/g from aqueous $AgNO_3$ (QE = 0.5%) at 450 nm[182]
85	Ag_3VO_4		300 W Xe at >420 nm	makes 17 μmol/h/0.3 g of O_2 from an aqueous $AgNO_3$ solution[183]
86a	WO_3		500 W Xe at >330 nm	O_2 rate (1220 μmol/h/g) in the presence of Fe^{3+} or Ag^+;[184] lower O_2 rates (38 μmol/h/0.8 g in the first hour) were measured by Arakawa and co-workers with $FeCl_3$ as the oxidizer together with traces (<0.7 μmol/10 h/0.8 g) of H_2[185]
86b	WO_3	Pt	300 W Xe at >420 nm	Pt−WO_3 alone with $NaIO_3$ produced O_2 at 84 μmol/h/0.2 g but no H_2; combined with Pt/$SrTiO_3$, H_2/O_2 evolved under vis light (420.7 nm) at rates of 0.21 and 0.11 μmol/h/0.4 g of both cats. (QE = 0.1%);[118,186] with TaON instead of $SrTiO_3$, H_2/O_2 rates of 24/12 μmol/h/0.4 g, QE = 0.4% at 420 nm[187]
87, **88**	$Na_2W_4O_{13}$, $Si(W_3O_{10})_4]^{4-}$		UV, 400 W Hg	21/9 μmol/h/g of H_2/O_2 from aqueous MeOH or Ag^+; in comparison, the protonated polytungstate ion $Si(W_3O_{10})_4]^{4-}$ with four H^+ produced H_2 (156 μmol/h/g) with methanol but no O_2[184]
89	Ca_2NiWO_6	Pt	UV, 300 W Xe	H_2 at 4.12 μmol/h/0.5 g from aqueous MeOH; from aqueous $AgNO_3$, O_2 is evolved at 0.38 μmol/h/0.5 g (0.36 μmol/h/0.5 g for vis light irradiation)[188]
90, **91**	$Bi_2W_2O_9$, Bi_2WO_6	Pt	UV, 450 W Hg	H_2 from MeOH(aq) at rates of 18 ($Bi_2W_2O_9$) and 1.6 (Bi_2WO_6) μmol/h/g; Bi_2WO_6 evolves 3 μmol/h/g of O_2 with vis light from an aqueous $AgNO_3$ solution[175]
92–94	Bi_2MoO_6, $Bi_2Mo_2O_9$, $Bi_2Mo_3O_{12}$		UV, 300 W Xe at >300 or >420 nm	all evolve O_2 from $AgNO_3$(aq) but no H_2 even from MeOH(aq); UV, low-temp (LT) modification of Bi_2MoO_6 (127 μomol/h/0.5 g), $Bi_2Mo_3O_{12}$ (46 μmol/h/0.5 g), $Bi_2Mo_2O_9$ (1.8 μmol/h/0.5 g), high temp modification of Bi_2MoO_6 (0.7 μmol/h/0.5 g); vis light, LT Bi_2MoO_6 (55 μmol/h/0.5 g), $Bi_2Mo_3O_{12}$ (7.6 μmol/h/0.5 g)[189]
95a/b	$PbMoO_4$, Cr:$PbMoO_4$		200 W Hg and 300 W Xe at >300 or >420 nm	from MeOH(aq), Pt/$PbMoO_4$ makes 59 μmol/h/0.3 g of H_2 under UV (Hg) and 3 μmol/h/0.3 g of O_2, but no H_2, from pure water; $AgNO_3$(aq), $PbMoO_4$ evolves 97 μmol/h/0.35 g of O_2 under UV (Hg);[190] under Xe UV light, the Cr-doped phases make up to 120 μmol/h/0.5 g of O_2 and up to 71.5 μmol/h/0.5 g of O_2 under vis light[191]
96	CeO_2		500 W Xe at >330 nm	using $Fe_2(SO_4)_3$ as the oxidizer, O_2 at ~2.5 μmol/h/0.8 g of cat.[185]

Table 1. Continued

no.	material	cocatalyst	irradiation conditions	reaction details and refs
97	ZrO_2		UV, 400 W Hg	72/36 μmol/h/g of H_2/O_2 from pure water; addition of $NaHCO_3$ increases the rate (309/167 μmol/h/g);[137] Pt, Cu, Au, or RuO_2 cocats. reduce the activity
98	Cu_2O		300 W Xe at >460 nm	H_2/O_2 at rates of 1.7/0.9 μmol/h/0.5 g of cat.;[192] activity partly due to mechanocatalysis[193]
99a/b	In_2O_3/Cr:In_2O_3	NiO, Pt	UV, 400 nm, Hg, or >420 nm, Xe	vis, 0.36/1.30 μmol/h/0.5 g of H_2/O_2 from MeOH(aq)/$AgNO_3$; UV, 1.1 μmol/h/0.5 g from pure water and no O_2;[194] for Cr:In_2O_3, the rates are lower
100a/b	$In_2O_3(ZnO)(m)$ (m = 3, 9)		300 W Xe at >420 nm	for m = 3, 1.1/1.3 μmol/h/g of H_2/O_2 from MeOH(aq)/$AgNO_3$ solution;[196] lower rates for m = 9
101	$Ba_2In_2O_5$	NiO, Pt	UV, 400 nm, Hg, or >420 nm, Xe	vis, 3.2/0.46 μmol/h/0.5 g of H_2/O_2 from MeOH(aq)/$AgNO_3$; UV, 4.2 μmol/h/0.5 g from pure water and no O_2; for Cr:$Ba_2In_2O_5$, the rates are lower; for $In_2O_3-Ba_2In_2O_5$, 7.8 μmol/h/0.5 g of H_2 from pure water (UV);[194] Cr doping gives 7.9/0.35 μmol/h/0.5 g of H_2/O_2 from MeOH(aq)/$AgNO_3$ (vis) and 29.3/15.2 μmol/h/0.5 g from pure water (UV)
102–104	MIn_2O_4 (M = Ca, Sr), $LaInO_3$	RuO_2	UV, 400 W Xe (280–700 nm) or 200 W Hg/Xe (230–436 nm)	$RuO_2-CaIn_2O_4$, H_2/O_2 at up to ~21/10 μmol/h/0.25 g of cat.; $RuO_2-SrIn_2O_4$, H_2/O_2 at rates of ~7/3.5 μmol/h/0.25 g; $RuO_2-LaInO_3$, ~1/0.5 μmol/h/0.25 g;[197] deviating yields in other references[200,260]
105	Zn:Lu_2O_3/Ga_2O_3	NiO	UV, 400 W Hg	50.2 μmol/h/0.5 g for H_2 and 26.7 μmol/h/0.5 g for O_2, respectively, with QE = 6.81% at 320 nm[198]
106	$ZnGa_2O_4$	RuO_2	UV, 200 W Hg/Xe	H_2 and O_2 from pure water with rates of ~10/~3.5 μmol/h/0.25 g of cat.[199]
107	Sr_2SnO_4	RuO_2	UV, 400 W Hg	H_2/O_2 evol. at 13/5 μmol/h/0.25 g from pure water[200]
108–111	$M_2Sb_2O_7$ (M = Ca, Sr), $CaSb_2O_6$, $NaSbO_3$	RuO_2	200 W Hg/Xe	H_2 (near stoich. O_2) at 2.8 ($Ca_2Sb_2O_7$), 7.8 ($Sr_2Sb_2O_7$), 1.5 ($CaSb_2O_6$), and 1.8 ($NaSbO_3$) μmol/h/0.25 g of cat.; no H_2 without RuO_2;[201] an earlier paper reports H_2/O_2 rates of 4.5/2.5 μmol/h/0.25 g for $NaSbO_3$[200]
112	Zn_2GeO_4	RuO_2	Hg/Xe (power not specified)	H_2 (22 μmol/h) and O_2 (10 μmol/h) from pure water (amount of cat. not specified)[202]
113	GaN:ZnO	RuO_2 or Cr/Rh oxide	UV, 450 W Hg at >300 nm and 300 W Xe at >400 nm	at pH = 3, H_2/O_2 at ~1/0.29 mmol/h/0.3 g; QE for O_2 evol. = 0.14% (for 300–480 nm) to 0.23% (for >420 nm)[203,204] with RuO_2 cocat.; with Cr/Rh cocat., QE = 2.5% at 420–440 nm[14,15,205]
114	β-Ge_3N_4	RuO_2	UV, 450 W Hg	stoich. H_2/O_2 at H_2 rates of ~0.5 mmol/h/0.5 g, QE = 9% at 300 nm; pure Ge_3N_4 is inactive[206,207]
115	$Zn_{1.44}GeN_{2.08}O_{0.38}$	RuO_2	UV, 450 W Hg at >400 nm	UV, H_2/O_2 rates of 54.3/27.5 μmol/h/0.2 g of cat.; no activity without RuO_2; under vis light (>400 nm), cat. evolves H_2/O_2 at 14.2/7.4 μmol/h/0.2 g;[208] ZnO or $ZnGeN_2$ alone do not split water with or without RuO_2 cocat.
116	Ta_3N_5	Pt	300 W Xe at >420 nm	H_2 at 1.8 μmol/h/0.2 g from MeOH(aq) (QE = 0.1% for 420–600 nm); O_2 at up to 100 μmol/h/0.2 g from $AgNO_3$(aq) with La_2O_3 buffer (pH = 8.5)[69,209]
117a	TaON	Pt or Ru	300 W Xe at >420 nm	O_2 at a rate of 380 μmol/h/0.4 g (QE = 34%) during the first hour from $AgNO_3$(aq) with La_2O_3 as a base buffer (pH = 8);[210] H_2 at 4 μmol/h (QE = 0.2%) with 0.4 g of Pt−TaON from MeOH(aq); Ru-TaON, 120 μmol/h/0.4 g of H_2 (QE = 0.8%)[44,211]
117b	TaON		300 W Xe at >420 nm	H_2/O_2 rates of 24/12 μmol/h/0.4 g (0.2 g of each cat.) in tandem with Pt−WO_3 and iodide as a redox shuttle (QE = 0.4% at 420 nm)[187]
118–120	$MTaO_2N$ (M = Ca, Sr, Ba)		300 W Xe at >420 nm	H_2 forms at 15–20 μmol/h/0.2 g from MeOH(aq); no O_2 from $AgNO_3$(aq)[44]
121	$LaTiO_2N$	Pt or IrO_2	300 W Xe at >420 nm	for Pt cocat., H_2/O_2 at ~8/29 μmol/h/0.2 g from MeOH(aq)/$AgNO_3$ (with La_2O_3 buffer for pH = 8) during the first 10 h; for H_2, QE = 0.15%; for IrO_2 as cocat., 200 μmol/h/0.25 g of O_2 (QE = 5%)[212]
122	$Y_2Ta_2O_5N_2$		300 W Xe at >420 nm	0.3 g of Pt/Ru-modified cat. evolves H_2 at 250 μmol/h from aqueous ethanol; the O_2 rate was 140 μmol/h/0.3 g from $AgNO_3$(aq) and La_2O_3 as a base buffer (pH = 8)[213]
123	InP	Pt	UV, 250 W Hg	H_2 at 2–5 μmol/h/30 mg of cat. from SO_3^{2-} (aq) or S^{2-}; cat. was not characterized[214]
124a	CdS	Pt	150 W Hg at >360 nm	1–10 μmol/h of H_2 for 5 mg of cat. with EDTA as the sacrif. donor; decomp. after >4 h[93,218,219]
124b	CdS, doped with ZnS and Ag_2S	Pt	900 W Xe at >300 nm or sunlight	Pt−CdS, up to 66 mL/h/0.4 g of cat. (=2.9 mmol/h), QE = 25% from aqueous S^{2-}, SO_3^{2-}, or S^{2-}/HPO;[217,220] QE = 37% for 15 mol % ZnS:CdS[217]
124c	CdS	Pt/RuO_2	450 W Xe at >400 nm	2.8 mL of H_2 (125 μmol) and 1.4 mL of O_2 per 44 h per 2.75 mg of cat. from pure water;[221,222] O_2 evol. was questioned [21,70,93]

Table 1. Continued

no.	material	cocatalyst	irradiation conditions	reaction details and refs
124d	CdS	variable	variable	micelles,[223–225] CdS composites with (TiO_2,[226] ZnS,[228,229] CdSe[230]) different cocats. (Pt, Pd, Rh, Ru, Ir, Fe, Ni, Co),[231,232] hollow CdS microparticles,[233] Cu-doped CdS,[234,235] effect of preparation[236,237]
125a	ZnS		125 W Hg at >290 nm	0.5 mL of H_2/h (22 μmol) per 12 mg of cat. from THF(aq)[238]
125b	ZnS	Pt	200 W Hg at >300 nm	295 mL/h (13 mmol/h) of H_2 from 0.4 g of cat., QE = 90%;[13] from aqueous S^{2-}, SO_3^{2-}, S^{2-}/HPO_2^-, or $S_2O_3^{2-}$ solution
125c	M:ZnS (M = Ni, Pb, Cu)		300 W Xe at >420 nm	M = Ni, 280 μmol/h/g (QE = 1.3%) of H_2 from aqueous K_2SO_3 and Na_2S;[240] M = Pb, 15 μmol/h/g from aqueous SO_3^{2-};[241] M = Cu, 450 μmol/h/g of H_2 were evolved (QE = 3.7%) from Na_2SO_3(aq)[239]
125d	ZnS, doped with $AgInS_2$ or $CuInS_2$	Pt or Ru	300 W Xe at >420 nm	for Ru-modified $(CuAg)_{0.15}In_{0.3}Zn_{1.4}S_2$, H_2 at up to 2.3 mmol/h/0.3 g from aqueous Na_2S and Ka_2SO_3 with QE = 7.5%;[243] Pt-loaded $(AgIn)_{0.22}Zn_{1.56}S_2$ has QE = 20%[245]
126–128	$Na_{14}In_{17}Cu_3S_{35}$, $(AEP)_6In_{10}S_{18}$, $Na_5In_7S_{13}$		300 W Xe at >420 nm	9 μmol/h/0.5 g of H_2 from Na_2S(aq) with QE = 3.7% (QE = 0.37% for SO_3^{2-}(aq)); $(AEP)_6In_{10}S_{18}$ evolved 20 μmol/h/0.5 g;[247] AEP = protonated 1-(2-aminoethyl)piperazine; $Na_5In_7S_{13}$ produced 2.4 μmol/h/0.25 g from Na_2SO_3(aq)[246]
129a/b	$[In(OH)_ySz]$ with or without Zn doping		300 W Xe at >420 nm	0.9–1.8 μmol/h/0.3 g from aqueous Na_2S/Na_2SO_3; for Pt/$In(OH)_ySz$:Zn, activity up to 67 μmol/h/0.3 g (QE = 0.59%) under similar condions[248]
130–132	$MInS_2$ (M = Cu, Na, $CuIn_5S_8$)		UV, 400 W Xe	$CuInS_2$ (0.006 mL/h/0.5 g of cat.) and $CuIn_5S_8$ (0.04 mL/h/0.5 g of cat.) from Na_2SO_3(aq);[249] $NaInS_2$−Pt produces H_2 (470 μmol/h/0.7 g) from K_2SO_3(aq);[250] under vis light (>420 nm, 300 W Xe).
133	WS_2		1000 W Xe at >435 nm	0.05 mL of H_2/h/10 mg of cat. from EDTA(aq) with fluoresceine as the sensitizer and SiO_2 as the support[251]
134	Bi_2S_3		500 W halogen lamp, vis	H_2 at 0.011 mL/h/0.001 g from aqueous sulfide; platinization improves the activity by 25%[252]

catalytic activity of these systems was found to strongly depend on the doping levels of the catalysts, the TiO_2 concentration, the pH, and the temperature.[90] Later it was discovered that O_2 production was less than stoichiometric[29] or entirely absent in some cases.[21,93] This was attributed to the fact that photoreduced TiO_2 tends to strongly adsorb oxygen as O_2^{-}[29,93] or as O_2^{2-}.[94] Following initial reports on the beneficial effect of a NaOH coating on the photocatalytic efficiency,[95] Arakawa's group reported in 1992 that the O_2 evolution activity of TiO_2[96] could be enhanced significantly by the addition of 0.1–2.2 M Na_2CO_3 to the aqueous catalyst dispersion. A similar effect was observed later for Ta_2O_5, ZrO_2, $SrTiO_3$, $K_4Nb_6O_{17}$, $Na_2Ti_2O_{13}$, and $BaTi_4O_9$.[40,41] On the basis of IR spectroscopy, the authors hypothesize that surface-adsorbed peroxycarbonate species are involved in facilitating O_2 release.[41] While Na_2CO_3 was found to also prevent the back-recombination of H_2 and O_2,[41] an alternative way to suppress this reaction is to substitute Pt in TiO_2/Pt catalysts with Pd and Rh.[95] The rate [h^{-1}] of the back-recombination reaction decreased in the order of Pd (0.23–0.51) > Pt (0.32–1.8) > Rh (0.20–0.30); however, Rh was also the least active cocatalyst for the forward reaction.[95] For certain niobates and tantalates (in particular, La-doped $NaTaO_3$), it was recently shown that H_2/O_2 back-recombination can be fully prevented with Au nanoparticles as cocatalysts.[97] However, for Au the reduction of O_2 takes place in competition with H_2O.

Unfortunately, the mechanism of photochemical reactions on the surface of TiO_2 has not yet been fully understood[78,98] and is subject to ongoing studies.[99–102] It is known though that irradiation with UV light produces electron–hole pairs, which become trapped after 250 ns (holes) and 20 ps (electrons) to produce absorptions in the visible at 475 nm (holes) and 650 nm (electrons), respectively.[103–105] Electrons can be trapped as Ti^{3+} ions,[105,106] which have been shown to be capable of reducing water to H_2.[78] Holes are trapped on surface hydroxyl sites,[81,104] which are believed to react with water to eventually produce O_2.

More recent work on TiO_2 water-splitting catalysts includes tandem systems with separate semiconductors for water reduction and oxidation (Figure 1D).[107] Under UV irradiation, Pt−TiO_2 (Anatase) was found to preferentially catalyze water reduction with iodide as the sacrificial electron donor, whereas TiO_2 (Rutile) was found to be the superior water oxidation catalyst in the presence of IO_3 as the electron acceptor. After both catalysts were combined, H_2 and O_2 were formed stoichiometrically from a basic (pH = 11) solution, with iodide serving as a redox shuttle. A similar system was realized with Pt−TiO_2 (Anatase) and Pt−WO_3, giving QE = 4% upon irradiation with UV light.[108] Other recent efforts have sought to improve the optical response of TiO_2-based catalysts via doping with C[109] or N[110,111] and S.[112] Of these materials, only N-doped TiO_2 has been tested for photocatalytic water splitting. Under visible light, the Pt-modified catalyst evolves O_2 from aqueous $AgNO_3$ as the sacrificial electron acceptor and traces of H_2 from aqueous methanol as the sacrificial electron donor.[113]

Titanates

When TiO_2 is fused with metal oxides (SrO, PbO, etc.), metal titanates with intermediate band gaps can be obtained.

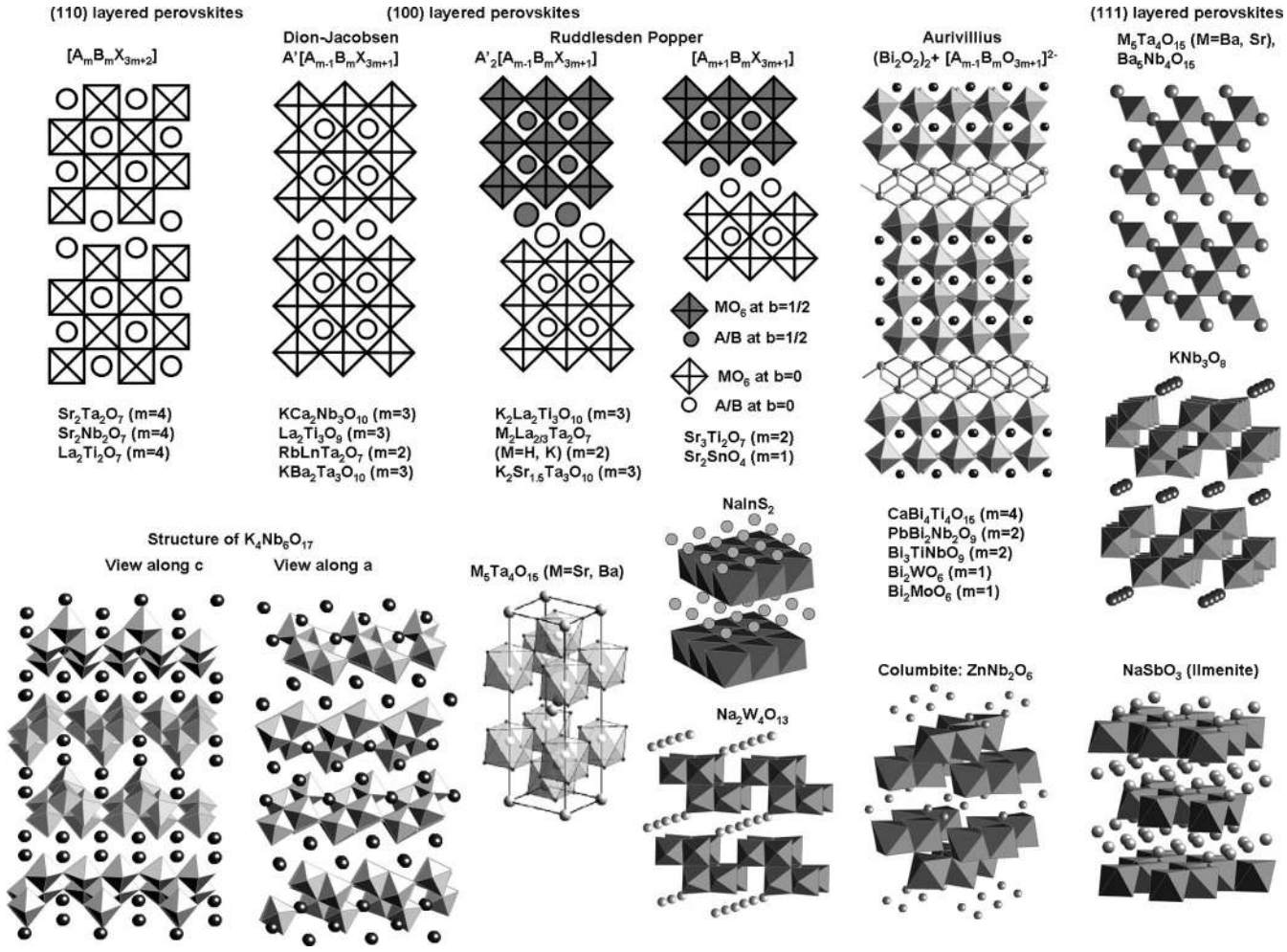

Figure 2. Crystal structures of layered semiconductors. For general structures ABX, A atoms are represented as spheres and BX units are shown as polyhedra.

Of these, $SrTiO_3$ crystallizes in the Perovskite structure type and has a band gap of 3.2 eV, slightly larger than that of TiO_2. It was first employed in 1976 as a photocatalyst in a water-splitting electrochemical cell together with p-CdTe or p-GaP photocathodes.[114] An optimized version of this system was shown in 1977 by Ohashi and co-workers to be the first self-supported photoelectrochemical cell[115] with a photon-to-electron conversion efficiency of 0.044−0.67%. In 1980, it was shown that NiO-modified $SrTiO_3$ powder splits water vapor stoichiometrically under UV irradiation, while $SrTiO_3$ alone did not show any activity.[116] The conditions of the NiO deposition had a strong effect on the catalytic activity.[117] Abe et al. used Cr/Ta-doped Pt/$SrTiO_3$ together with Pt−WO_3 in a two-particle catalyst system (z scheme, Figure 1D) for overall water splitting with visible light. Here Cr/Ta:$SrTiO_3$−Pt produced H_2 and Pt−WO_3 produced O_2, with an iodide/iodate redox couple serving as the redox mediator between the two catalysts.[118] The effect of metal cocatalysts (Ru, Ir, Pd, Pt, Os, Re, Co) on the water-splitting activity of $SrTiO_3$ was studied by Lehn et al.[119,120] From pure water, H_2 and O_2 were evolved stoichiometrically, with the activity decreasing in the order Rh > Ru > Re > Pt > Ir > Pd > Os > Co. $SrTiO_3$ alone produced H_2 but no O_2. Lee and co-workers investigated a series of layered Perovskites as photochemical water-splitting catalysts.[121,122] $La_2Ti_2O_7$ is a member of the (110)-layered Perovskites $[A_mB_mX_{3m+2}]$ with $m = 4$ (Figure 2); i.e., it consists of four TiO_6 unit thick slabs that are separated by layers of La^{3+} ions. Because of its large band gap of 3.8 eV,[123] it requires UV irradiation for catalytic activity. The NiO-modified catalyst is active for H_2/O_2 evolution with a QE up to 12%.[121−123] By doping with BaO and addition of NaOH to the catalyst suspension, this activity could be further increased to QE = 50%,[121] only slightly below that of the best catalyst, La-doped $NaTaO_3$ (56%, see below).[12] With Pt as a cocatalyst, the activity is substantially lower.[124] A hydrothermally synthesized material with larger surface area exhibits intermediate activity.[125] Doping of $La_2Ti_2O_7$ with Cr or Fe does not increase the H_2 activity under UV irradiation but allows H_2 production (<15 μmol/h for Pt−Cr:$La_2Ti_2O_7$) from aqueous methanol with visible light.[124] $La_2Ti_3O_9$ is a (100)-layered Perovskite with $m = 3$ (Figure 2). Under UV irradiation, the NiO-modified catalyst splits water at significantly lower rates than $La_2Ti_2O_7$.[121] The activity of La_2TiO_5 is slightly higher, even though the material does not form a layered structure. Instead, it contains corner-shared chains of TiO_5 pyramidal units (Figure 3).[121] $Sr_3Ti_2O_7$ is a (100)-layered Perovskite of the Ruddlesden–Popper series $[A_{m+1}B_mX_{3m+1}]$ with $m = 2$ (Figure 2). From its absorption edge at 395 nm, its band gap can be estimated as 3.2 eV. Under UV irradation, it produces only H_2 from water, but stoichiometric O_2 evolution can be achieved after modification with a NiO cocatalyst.

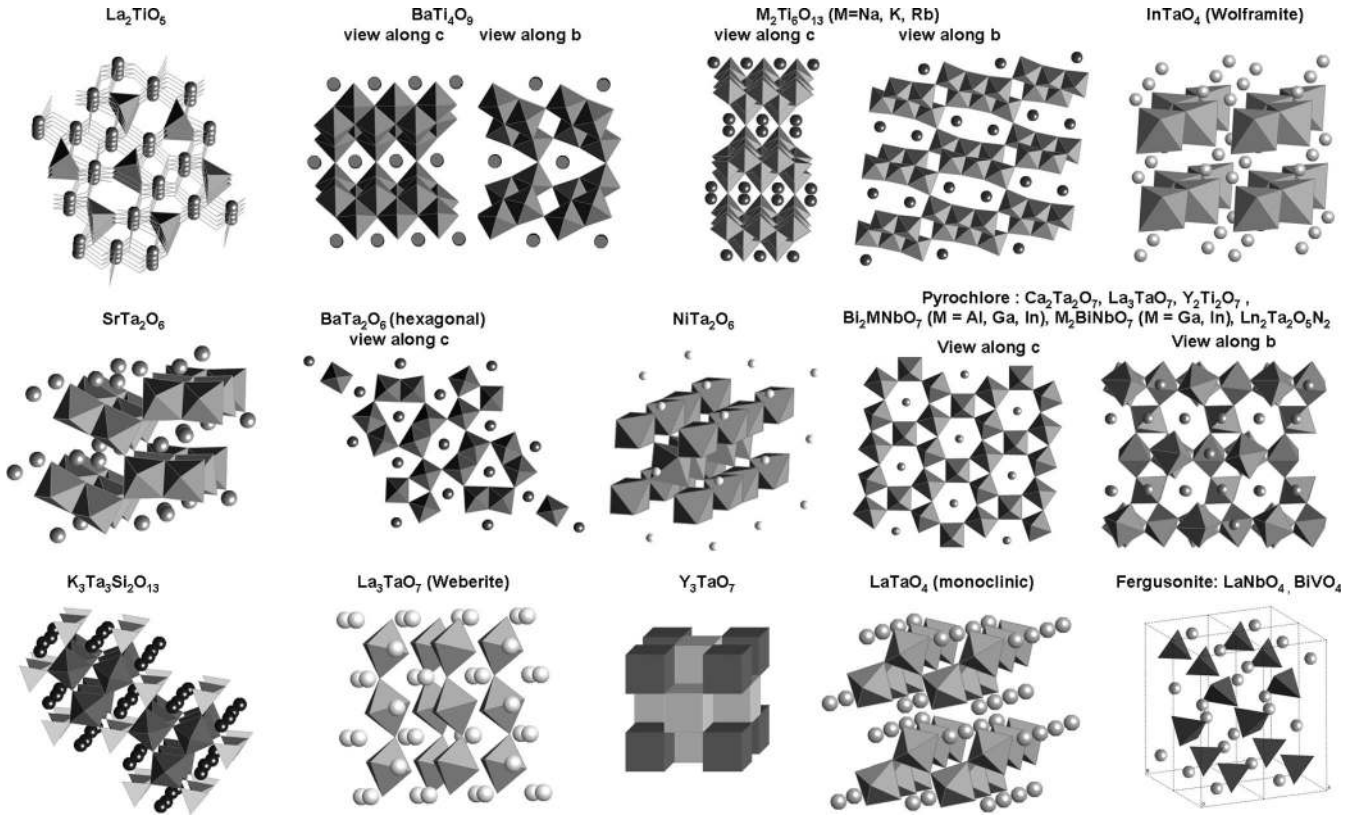

Figure 3. Crystal structures of semiconductors (part I). For general structures ABX, A atoms are represented as spheres and BX units are shown as polyhedra.

An alternate synthetic route produces a high-surface-area material with increased activity, after modification with NiO.[126] Doping of $Sr_3Ti_2O_7$ with Pb^{2+} cations leads to $PbTiO_3$ (Perovskite structure, not shown) with a reduced band gap of 2.98 eV.[127] After modification with Pt nanoparticles, visible light activates the catalyst to produce H_2 from aqueous methanol and O_2 from aqueous $AgNO_3$. Doping of $Sm_2Ti_2O_7$ with sulfur produces $Sm_2Ti_2S_2O_5$, which belongs to the Ruddlesden–Popper-type (100)-layered Perovskites with $m = 2$ and with S occupying O sites. The semiconductor has a reduced band gap of 2.0 eV, from optical measurements. Under visible light irradiation, the Pt-modified catalyst produces H_2 in the presence of $Na_2S-Na_2SO_3$ or methanol but not from pure water. After modification with IrO_2 and $Ca(OH)_2$, O_2 evolution proceeds in the presence of 0.01 M of the oxidizing agent $AgNO_3$.[128] After NiO functionalization and doping of up to one Nb^{5+} on the Ti^{4+} sites, the Ruddlesden–Popper series ($m = 3$) $M_2La_2Ti_3O_{10}$ (M = K, Rb, Cs) cleaves water into H_2 and O_2 with QEs of up to 5%.[129,130] The activity of $K_2La_2Ti_3O_{10}$ (shows photoluminescence at 475 nm at 77 K)[131] is strongly dependent on the cocatalyst (Ni, Pt, or RuO_2, Au [132]) and on the concentration of added KOH.[133] It can be doubled by synthesizing the catalyst under conditions that produce submicrometer crystals.[134] As a member of the Aurivillius-type layered Perovskites ($m = 4$), $CaBi_4Ti_4O_{15}$ consists of quadruple-layer TiO_6 sheets separated by layers of $[Bi_2O_2]^{2+}$ (Figure 2). Substitution of Ca^{2+} with Pb^{2+} reduces the band gap of the material from 3.36 to 3.02 eV. Under visible light, the resulting $PbBi_4Ti_4O_{15}$ evolves small quantities of H_2 and O_2 from aqueous MeOH and $AgNO_3$, respectively.[127] Inoue studied the photocatalytic properties of a series of titanates ($BaTi_4O_9$, $Ba_4Ti_{13}O_{30}$, $Ba_2Ti_9O_{20}$, $Ba_6Ti_{17}O_{40}$), whose structures contain tunnels occupied by alkaline-earth metal ions.[42] Upon UV irradiation, only $BaTi_4O_9$ (Figure 3) was able to split water stoichiometrically into H_2 and O_2 after modification with RuO_2. The activity of this catalyst was attributed to the presence of distorted TiO_6 octahedra whose stronger dipole moments aided electron–hole separation. In the related series $M_2Ti_6O_{13}$ (M = Na, K, Rb) (Figure 3) the tunnels are twice as large. After modification with RuO_2 particles, all members of the series produced H_2/O_2 from water, with the activity increasing with decreasing size of the cation.[42,135] This trend was correlated with the sizes of the dipole moment in these structures originating from distorted TiO_6 octahedra. An additional factor was that <1 nm RuO_2 particles were thought to be able to make good electrical contact with the titanates, by fitting into the opening of the tunnel voids. $La_4CaTi_5O_{17}$ is a member of the 110-layered Perovskites $[A_mB_mO_{3m+2}]$ with $m = 5$ (Figure 2) and has a band gap of 3.8 eV. After modification with NiO, this catalyst was active for an overall water splitting under UV light with a QE of up to 20%.[122]

Noncrystalline Ti/Zr phosphates were also explored as catalysts for photochemical water splitting. The polymerization of titanium and zirconium tetraisopropanolates in aqueous H_3PO_4 in the presence of octadecyltrimethylammonium chloride produces a series of amorphous Ti/Zr phosphates, which after modification with Pt metal evolve H_2 from water under UV light.[136] The activity increases with the Zr content to reach a maximum at a Ti/Zr molar ratio of 1:1.

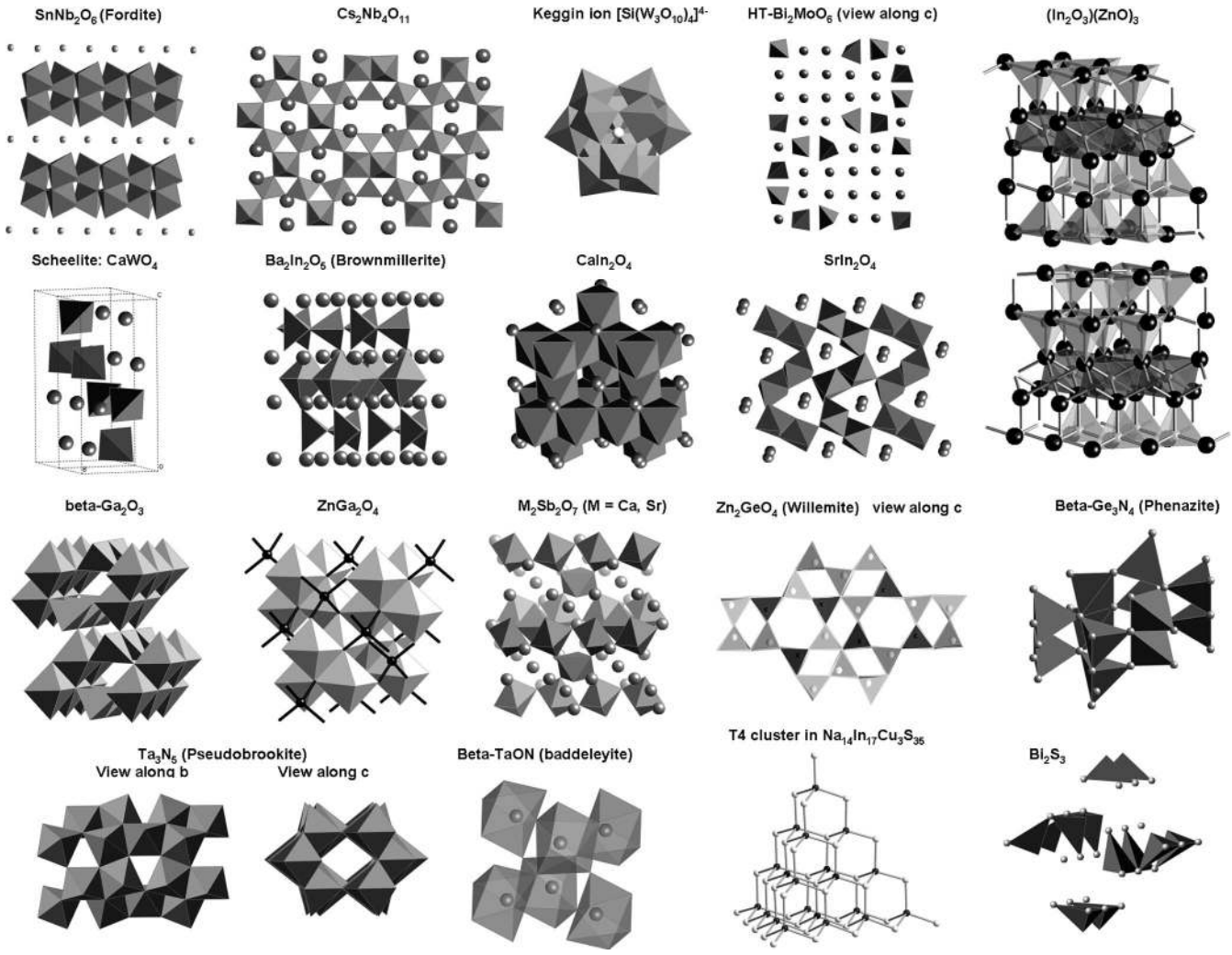

Figure 4. Crystal structures of semiconductors (part II). Continued from Figure 3.

Zirconium Oxide

ZrO_2 crystallizes in the Rutile structure type, like TiO_2, but its band gap of 5.0–5.7 eV[137,138] is much larger. Under UV irradiation, pure ZrO_2 is an active catalyst for overall water splitting. The rate can be optimized by the addition of alkali carbonates to the water, of which $NaHCO_3$ works best.[137] Interestingly, the addition of Pt, Cu, Au, or RuO_2 as cocatalysts reduces the activity below the value observed in pure water. This is explained with the large bandgap and the positions of the conductance band and valence bands respectively, which lead to a large barrier height of the metal semiconductor junctions.

Tantalum Oxide and Tantalates

Tantalum oxide and the tantalates form another large group of water splitting catalysts. Because of their large bandgaps UV irradiation is needed for activity, and in many cases, metal or metal oxide cocatalysts. The bandgap of Ta_2O_5 (3.9–4.0 eV) lies between that of ZrO_2 (5.0 eV), and TiO_2 (3.0 eV). By itself it produces only traces of H_2 and no O_2 in pure water upon UV illumination. However, the addition of NiO, Pt, or RuO_2 cocatalysts converts the material into an active water-splitting catalyst (see Table 1).[40,48] The crystal structure of Ta_2O_5 is not known, but first-principle calculations suggest a hexagonal structure containing hexa- and octacoordinate Ta ions.[139] The first layered tantalates $A_4Ta_xNb_{6-x}O_{17}$ ($A = Rb, K$; $x = 1-4$) were synthesized by doping $K_4Nb_6O_{17}$ with Ta_2O_5 by Domen et al. in 1996.[140] These compounds are isomorphous with $K_4Nb_6O_{17}$ (see Figure 2). The band gaps in the series increase with the Ta content from 3.4 eV for $Rb_4Nb_6O_{17}$ to 4.2 eV for $Rb_4Ta_6O_{17}$, except for $K_4Ta_4Nb_2O_{17}$ whose absorption edge at 410 nm revealed a band gap of only 3.0 eV. After modification with NiO, all materials split water under UV irradiation, but the activity decreases with increasing Ta content. Kato and Kudo discovered in 1998 that tantalates $MTaO_3$ ($M = Li, Na, K$) are also very effective photocatalysts for water splitting under UV irradiation.[48,141] The oxides crystallize in the Perovskite structure type, and their band gaps depend strongly on the cations, 4.7 eV (Li), 4.0 eV (Na), and 3.7 eV (K), as determined from diffuse-reflectance spectra.[142] In combination with NiO as the cocatalyst, $NaTaO_3$ produced H_2 and O_2 from pure water with quantum yields of 20–28%.[141,142] Without cocatalysts, the rates for H_2/O_2 production are 10–40 times lower, depending on the experimental conditions.[142] Recent work by Teng and co-workers showed that $NaTaO_3$ produced by a sol–gel method showed higher activity for water splitting than the same material prepared by a high-temperature (HT) solid-state synthesis.[143] This was attributed

to the higher surface area of the sol–gel product and to its monoclinic crystal structure (instead of orthorhombic) with a slightly larger band gap (4.1 eV). In 2003, Kudo and co-workers reported that $NaTaO_3$, doped with 2 mol % La and modified with a NiO cocatalyst, split pure water with a quantum yield of 56% under UV irradiation.[12] This is the highest QE ever reported for a water-splitting catalyst. The high performance was attributed to the La dopant, which reduced the catalyst particle size and caused the formation of nanosteps on the particle surface. According to the authors, the grooves in the nanosteps served as O_2 formation sites, while NiO particles at the step edges catalyzed H_2 formation. The related $La_{1/3}TaO_3$ (4.0 eV), on the other hand, has significantly lower activity with a NiO cocatalyst.[144] Doping of $KTaO_3$ with Ti, Zr, and Hf also increases its water-splitting activity but not above that of NiO−La:$NaTaO_3$.[145] Ti works best (at 8% doping level), followed by Zr and Hf. The cation size of the dopant could be correlated with the distortion of the structure and the O_2 production rate and inversely with the H_2 production rate. Zr:$NaTaO_3$ crystals coated with metal porphyrinoids and with Pt particles were found by Ishihara and co-workers to catalyze water splitting under UV irradiation with QEs of up to 12.8%.[146] The photocatalytic activity depended strongly on the nature of the porphyrin ligand and also on the metal cation (Zn, Co, Cr, Mg). Time-resolved measurements of the photovoltaic potential showed that the porphyrin prolongs the half-life of the excited state from 4.0 to 11.2 μs. It was suggested that the porphyrin complex aids the transport of the photexcited electron to the Pt cocatalyst, the site of water reduction. Water splitting under visible light irradiation was achieved by Arakawa's group with Ni-doped $InTaO_4$ modified with RuO_2 or NiO as the cocatalyst.[47,62] $InTaO_4$ forms a Wolframite type structure consisting of zigzag chains of edge-shared TaO_6 octahedra (see Figure 3). The Ni^{2+} ions displace In^{3+} from its sites, leading to a contraction of the lattice. The partially filled Ni d-orbitals reduce the band gap of the material from 2.6 to 2.3 eV and cause absorption at 480 nm in the visible. The best catalyst produced H_2/O_2 from pure water under visible irradiation with QE = 0.66% and without deterioration in the activity. Under similar conditions, nondoped NiO−$InTaO_4$ was 5 times less active. The water-splitting properties of the alkaline-earth tantalates were studied by various researchers.[147–149] $SrTa_2O_6$ consists of edge- and corner-shared TaO_6 octahedra (Figure 3) and has a band gap of 4.5 eV based on its absorption edge at 280 nm.[149] from pure water with QE = 7%.[147–149] $BaTa_2O_6$ crystallizes in three modifications (hexagonal, 4.0 eV, shown in Figure 3; tetragonal, 3.8 eV; orthorhombic, 4.1 eV), of which the orthogonal phase shows the highest photocatalytic activities for overall water splitting because it has the largest band gap.[48] The addition of NiO cocatalysts and of a small amount of $Ba(OH)_2$ strongly enhanced the photocatalytic reaction. $NiTa_2O_6$ (network of corner-shared TaO_6 octahedra; Figure 3) also produced both H_2 and O_2 without cocatalysts, whereas $MnTa_2O_6$, $CoTa_2O_6$, $CrTaO_4$, and $FeTaO_4$ made only traces of H_2.[48] $Ca_2Ta_2O_7$ has a Pyrochlore structure consisting of a 3D network of corner-shared TaO_6 octahedra (Figure 3). It showed very good activity for overall water splitting when loaded with a NiO cocatalyst. The phases Bi_2MTaO_7 (M = La, Y) also crystallize in the Pyrochlore structure type, with the lanthanide ions partially occupying Ta^{5+} sites. Based on diffuse-reflectance spectra, the band gaps of these semiconductors are 2.17 eV for M = La and 2.22 eV for M = Y. Under UV irradiation, Bi_2LaTaO_7 was the slightly more active catalyst, producing H_2/O_2 from pure water.[150] As a Ruddlesden–Popper layered Perovskite with $m = 4$, $Sr_2Ta_2O_7$ is a fairly active catalyst for the overall splitting of water with NiO as the cocatalyst.[149,151] Because of its larger band gap (4.6–4.8 eV), it is more active than the related $Sr_2Nb_2O_7$. The compounds $M_2La_{2/3}Ta_2O_7$ (M = H, K) and $H_2SrTa_2O_7$ are Ruddlesden−Popper layered Perovskites $m = 2$ (Figure 2) separated by layers of K^+ or H^+ ions. The band gaps of these materials are 3.9–4.0 eV, based on the optical absorption edge around 320 nm. Upon UV irradiation, the NiO-modified catalysts split water into H_2/O_2. The activity increases in the order $H_2SrTa_2O_7$ < $K_2La_{2/3}Ta_2O_7$ < $H_2La_{2/3}Ta_2O_7$, with the high rates for NiO−$H_2La_{2/3}Ta_2O_7$ attributed to efficient NiO and Ni^{2+} intercalation into the interlayer space. Without NiO, the rates are about half, except for $H_2SrTa_2O_7$, which is more active in the pure form.[144] $K_2Sr_{1.5}Ta_3O_{10}$ belongs to the layered Ruddlesden−Popper phases with $m = 3$ (Figure 2). Its absorption edge occurs at 300 nm, and its band gap is estimated as 4.1 eV. At 77 K, it exhibits a luminescence peak at 404 nm. After modification with RuO_2, the catalyst has modest activity toward overall water splitting (QE = 2%) under UV light. Without a cocatalyst, the activity is ~6 times lower.[152] Under analogous conditions, the 100-layered Perovskite $KBa_2Ta_3O_{10}$ (Figure 2) achieves a QE of 8% after modification with NiO.[122] High surface modifications of $Sr_4Ta_2O_9$ (cubic Perovskite with Sr on 50% of the Ta sites, not shown) and of the (111)-layered Perovskite $M_5Ta_4O_{15}$ (M = Sr, Ba) (Figure 2) were synthesized by calcination of a mixture of the metal ions, citrate, ethylene glycol, and methanol.[149] Their band gaps are 4.8 eV from the respective absorption edges (260 nm). All NiO-modified materials catalyze H_2/O_2 evolution from pure water, with $Ba_5Ta_4O_{15}$ (3.9 eV) having the highest activity when a small amount of $Ba_{0.5}TaO_3$ is present.[153] $K_3Ta_3Si_2O_{13}$ contains chains of corner-linked TaO_6 octahedra, cross-linked by Si_2O_7 ditetrahedral units (Figure 3). A luminescence at 500 nm (77 K) is probably due to a defect emission, and the band gap is estimated as 4.1 eV based on UV/vis. Under UV illumination, the compound produces small amounts of both H_2 and O_2, but NiO loading improves the activity by a factor of 10.[154] The crystal structure of $K_3Ta_3B_2O_{12}$ is very similar, except that the Si_2O_7 units are replaced by double sets of planar BO_3 units (structure not shown). The larger band gap of 4.2 eV (from UV/vis, luminescence at 432 nm) is attributed to distortions of the TaO_6 octahedra with *trans*-O−Ta−O bond angles of 171.5°, compared to 173° in $K_3Ta_3Si_2O_{13}$. Under UV irradiation, the catalyst is very active toward water splitting but addition of NiO does not improve the activity.[155] In 2004, Arakawa's group studied the effect of the crystal structure on the catalytic activity for a series of tantalates M_3TaO_7 with M = Y, Yb, Gd, La.[156] For La_3TaO_7 (4.6 eV), it was found that the orthorhombic Weberite modification had a much higher activity than the

cubic Pyrochlore structure, despite the same band gap.[123] The Weberite structure type contains chains formed by corner-shared TaO_6 octahedra (Figure 3), whereas the Pyrochlore structure has a 3D network of corner-shared TaO_6 octahedra (Figure 3). For R = Y, Yb (structure contains alternating TaO_8 and LnO_8 cubes; Figure 3) and Gd (Pyrochlore structure, Gd on every second Ta site, not shown), only trace amounts of H_2 were observed. These latter three structures lack TiO_6 chains, which seem necessary for efficient charge transport to the surface of the materials and photocatalytic activity. The tantalates $LnTaO_4$ (Ln = La, Ce, Pr, Nd, Sm) crystallize in the monoclinic $LaTaO_4$ type for Ln = La, Ce, Pr, or the monoclinic $LaNbO_4$ type (Fergusonite) for Ln =Nd, Sm. The structure of the former consists of corner-shared TaO_6 octahedra forming zigzag strings (Figure 3), while the Fergusonite ($BiVO_4$) structure is a distorted Scheelite ($CaWO_4$) structure, consisting of TaO_4 tetraedra separated by La^{3+} ions (Figure 3). The band gaps depend strongly on the nature of the lanthanide ion and vary from 2.4 (Cd) to 3.9 (Nd). Under UV irradiation, only NiO-modified $LaTaO_4$ has significant catalytic activity for H_2/O_2 evolution from water. The low activities of the other catalysts (they evolve traces of H_2) are explained with trapping of electrons in empty f levels just below the conduction band and with the absence of efficient charge-transport pathways in the case of the Fergusonite structure type.[157] The compounds $RbLnTa_2O_7$ (Ln = La, Pr, Nd, Sm) are (100)-layered Perovskites of the Dion−Jacobsen series (Figure 2) with $m = 2$ and with band gaps of 3.8–3.9 eV. In addition to the absorption edge at 300 nm, the optical spectra contain sharp absorptions above 300 nm, due to f−f transitions. Under UV irradiation, these catalysts have low activity for the total water splitting, but they improve upon the addition of a NiO cocatalyst. Exchange of Rb^+ with Na^+ reduces the rate significantly.[158,159]

Niobium Oxide and Niobates

While Nb_2O_5 is not an active photocatalyst for water splitting,[160] many niobates do split water upon UV irradiation. One of the best studied catalysts, $K_4Nb_6O_{17}$, was first discovered by the Domen laboratory in 1986.[160] The layered compound consists of Nb_6O_{17} sheets (Figure 2) held together by K ions. The sheets are composed of edge- and corner-shared NbO_6 octahedra and the material has a band gap of 3.3 eV. By itself, $K_4Nb_6O_{17}$ catalyzes nonstoichiometric water splitting at a low rate. Stoichiometric H_2/O_2 evolution is possible after modification with 0.1 wt % NiO, with efficiencies of 5.3–20% under optimized conditions,[122,161–163] e.g., by the addition of KOH/NaOH to the $Ni(NO_3)_2$ solution prior to calcination, leading to larger NiO clusters.[162] In comparison, the QE of NiO−$Rb_4Nb_6O_{17}$ is 10%.[43] When $K_4Nb_6O_{17}$ was internally platinized by ion exchange with $[Pt(NH_3)_4]^{2+}$ followed by reduction, the catalyst produced H_2/O_2 with QE = 1.3%. If Pt was *not* removed from the crystal surface, the activity was ~10 times lower because it catalyzed the back-reaction of H_2 and O_2.[164] Treatment of $K_4Nb_6O_{17}$ with propylammonium hydrochloride followed by reaction with a soluble titanium(4+) acetate gave a $K_4Nb_6O_{17}$−TiO_2 composite with low activity for an overall water splitting.[165] The excited-state dynamics for $K_4Nb_6O_{17}$ were investigated with transient absorption spectroscopy. Excitation with femtosecond pulses at 266 nm produces a broad transient absorption at 450–700 nm, belonging to photochemically generated charge carriers. The charge carriers recombine following second-order kinetics over the course of 1 ns.[166] Partial exchange of K^+ in $K_4Nb_6O_{17}$ with Ni^{2+} or H^+ does not affect the transient absorption spectra, suggesting that interfacial NbO groups are not involved in the excitation process.[167] Both $K_4Nb_6O_{17}$ and the related layered oxides KNb_3O_8, $KTiNbO_5$, and $CsTi_2NbO_7$ (KNb_3O_8 shown in Figure 2) also catalyze H_2 evolution from an aqueous HI solution. After internal platinization, cation−proton exchange, and sensitization with $[Ru(bpy)_3]^{2+}$ complexes (bpy = 2,2′-bipyridyl derivative), they produce small amounts of H_2 under visible irradiation, with $K_2H_2Nb_6O_{17}$ being the most active catalyst (QE = 0.3%).[74,168] The low efficiency in these systems is due to competition of the formed I_3^- for electrons. The use of (100)-layered Perovskites of the Dion−Jacobsen series $A'[A_{n-1}B_nO_{3n+1}]$ (A = K, Rb, Cs; B = Ca, Sr, Na, Pb; m = 2–4) as a water-splitting catalyst was first reported in 1990 by Domen's group.[169] These materials consist of double or triple layers of corner-shared NbO_6 octahedra with A ions located in the metal oxide layers and A′ ions between them (Figure 3). From absorption spectroscopy, the band gaps of these materials are estimated as 3.3–3.5 eV.[38,43] Under UV irradiation and using methanol as a sacrificial donor, the Pt-modified catalysts produce only small quantities of H_2 and no O_2,[169] but the catalytic activity increases dramatically after exchange of the alkaline-metal ions with protons. $HCa_2Nb_3O_{10}$ produces 5.9 mmol/h/g, and after modification with Pt, the rate increases to 19 mmol/h/g. The effect of cation exchange on the increase in the catalytic activity is attributed to the widening of the interlayer gap to 0.08 nm and the incorporation of water into the interlayer space. Long-chain aliphatic alcohols like ethanol or propanol cannot enter this space and consequently diminish H_2 production.[169] Very recently, Ebina and co-workers reported that, under UV irradiation, $KCa_2Nb_3O_{10}$ had some activity for H_2 production from pure water (no O_2 was evolved) and medium activity for total water splitting after intercalation of RuO_x between the layers.[170] Treatment of $HCa_2Nb_3O_{10}$ with alkylamines followed by treatment with tetraethoxylsilane produced a $HCa_2Nb_3O_{10}$−SiO_2 composite with good activity for H_2 evolution from aqueous methanol. Added Pt further increased the activity. Because of the increased interlayer space, longer-chain alcohols could serve as efficient electron donors.[171] The activity of $KCa_2Nb_3O_{10}$ could also be enhanced significantly by restacking exfoliated $HCa_2Nb_3O_{10}$ nanosheets with KOH or NaOH, producing a material with 10 times greater specific surface area.[172] When Pt particles were intercalated, the restacked catalyst evolved H_2 10 times faster from an aqueous methanol solution than Pt-surface-modified $KCa_2Nb_3O_{10}$. When RuO_2 was intercalated, water was split stoichiometrically at a medium rate.[170] The water-splitting activity and the excited-state dynamics of exfoliated $HCa_2Nb_3O_{10}$ nanosheets were studied by Osterloh and co-workers.[173] After excitation at 300 nm, electrons and holes recombine over the course of nanoseconds

following second-order kinetics. Under UV irradiation, the nanosheets evolve only low H_2 rates from water (QE = 0.22%), but the growth of Pt nanoparticles on the nanosheets enhances the catalytic activity more than 30 times (QE = 7.5%). Doping of the Dion−Jacobsen phase $K_{0.5}La_{0.5}Ca_{1.5}Nb_3O_{10}$ (3.44 eV) with PbO/Bi_2O_3 gives $K_{0.5}La_{0.25}Bi_{0.25}Ca_{0.75}Pb_{0.75}Nb_3O_{10}$ with a band gap of 3.06 eV. After modification with Pt nanoparticles, the catalyst produces traces of H_2 from aqueous methanol and medium rates of O_2 from aqueous $AgNO_3$ under visible light irradiation.[127] The smaller band gap (2.5 eV) of the isomorphous $RbPb_2Nb_3O_{10}$ allows visible light absorption at <500 nm. After modification with Pt, only traces of H_2 are evolved from aqueous methanol, but protonation and internal platinization enable good H_2 rates.[174] $PbBi_2Nb_2O_9$ is a member of the Aurivillius-type layered Perovskites with $m = 2$ (Figure 2). Its band gap is 2.88 eV, judged from the visible absorption edge at 431 nm. Under visible light, the Pt-loaded catalyst produces small rates of H_2 (QE = 0.95%) from aqueous methanol and large rates of O_2 (QE = 29%) from aqueous $AgNO_3$.[113] For the isostructural Bi_3TiNbO_9, higher H_2 but lower O_2 rates are observed under UV irradiation.[175] Similar to the tantalates, the niobates Bi_2MNbO_7 (M = Al, Ga, In) crystallize in the Pyrochlore structure type (Figure 3) and have band gaps of ~2.7–2.9 eV.[47,176] Under UV irradiation, they evolve H_2 from aqueous methanol and O_2 from a $Ce(SO_4)_2$ solution at rates up to 710 and 25 μmol/h/g, respectively. The catalyst with M = Al is the most active. In contrast, the compounds M_2BiNbO_7 (M = Ga, In, Pyrochlore structure) have the ability to split water stoichiometrically under UV irradiation. The enhanced reactivity is observed despite the fact that the band gaps of these compounds are smaller (2.5–2.6 eV) than those for the series Bi_2MNbO_7.[177] $ZnNb_2O_6$ crystallizes in the columbite structure type containing double layers of edge- and corner-shared NbO_6 octahedra (Figure 3).[178] Under band-gap (4.0 eV) irradiation, it produces small amounts of H_2 but no O_2. Using a NiO cocatalyst, near-stoichiometric water splitting at a low rate can be achieved.[178] $SnNb_2O_6$ (Figure 4) forms the layered Fordite structure consisting of double layers of edge-shared NbO_6 octahedra separated by layers of Sn^{2+} ions. It has an absorption edge at 540 nm and a band gap of 2.3 eV. After modification with Pt, it evolves small amounts of H_2 from an aqueous methanol solution under visible light.[179] The isostructural $SnTa_2O_6$ is not active under these conditions but evolves small amounts of H_2 under UV irradiation. $Sr_2Nb_2O_7$ (3.9 eV from UV/vis) belongs to the Ruddlesden–Popper layered Perovskites with $m = 4$ (Figure 2). With NiO, the material splits water into H_2/O_2 with medium activity, while without NiO, only H_2 is produced.[151] QEs of up to 23% were observed by Lee and co-workers.[122] The isostructural $Ca_2Nb_2O_7$ (4.3 eV) produced H_2 with QE = 7% after modification with NiO (the O_2 rate was not determined).[122] $Cs_2Nb_4O_{11}$ has a complex structure containing corner- and edge-shared NbO_6 octahedra and NbO_4 tetrahedra (Figure 3). Despite its large band gap of 3.7 eV, it emits a blue photoluminescence at 440 nm at 77 K. Depending on the temperature for NiO coating, the catalyst can reach activities as high as $K_4Nb_6O_{17}$.[180] $Ba_5Nb_4O_{15}$ is a (111)-layered Perovskite containing layers of four NiO_6 octahedra thick slabs separated by Ba^{2+} cations (Figure 2). Its absorption edge lies at 322 nm (the band gap is 3.9 eV), and at 77 K it produces a broad photoluminescence at 532 nm. Its excellent activity for water splitting under UV light irradiation could be optimized further by increasing the surface area of the catalyst using a modified synthesis.[181] The isostructural tantalates are also excellent catalysts for overall water splitting.[149,153]

Other Transition Metal Oxides

Other transition metal oxides catalyze partial water redox reactions with the aid of suitable electron donors or acceptors. Fergusonite, $BiVO_4$, consists of VO_4 tetrahedra separated by Bi^{3+} cations (Figure 3). With a 2.3 eV band gap, it shows some activity for O_2 evolution from aqueous solutions of $AgNO_3$ under visible light irradiation.[182] Ag_3VO_4 also contains MO_4 tetrahedral units (structure not shown) and has a band gap of 2.0 eV and an absorption edge at 570 nm. Under visible light illumination, it evolves O_2 from an aqueous $AgNO_3$ solution at good rates.[183] WO_3 (2.8 eV) crystallizes in the ReO_3 structure type (not shown). In the presence of Fe^{3+} or Ag^+ ions, it can oxidize water at fairly high rates but not reduce it. In the presence of methanol, WO_3 bronze forms instead of H_2.[184,185] Pt-modified WO_3 was also used by Abe et al. in a tandem system with Cr/Ta-doped Pt-$SrTiO_3$ for an overall water splitting.[118,186] Under visible light irradiation, Pt−WO_3 alone with $NaIO_3$ produced O_2 at a high rate but no H_2. Combined with Pt/$SrTiO_3$ and using iodide as a redox shuttle, water splitting was observed under monochromatic light (420.7 nm) with small H_2/O_2 rates of 0.21 and 0.11 μmol/h for 0.4 g of both catalysts (QE = 0.1%). When Pt/$SrTiO_3$ was replaced with TaON (see below), QE increased to 0.4%.[187] The tungstate $Na_2W_4O_{13}$ forms a layered solid composed of two WO_6 octahedra thick sheets separated by Na ions (Figure 2). Under UV light, the material has good activity for H_2 evolution from aqueous MeOH and for O_2 evolution from aqueous $AgNO_3$.[184] In comparison, the Keggin ion $[Si(W_3O_{10})_4]^{4-}$ (Figure 4), a homogeneous catalyst, produces high rates of H_2 from aqueous methanol but no O_2 even when $AgNO_3$ is present.[184] Apparently, the clusters lack active sites for O_2 evolution. Ca_2NiWO_6 (structure not shown) crystallizes in the Perovskite structure, with Ni^{2+} and W^{6+} ions occupying positions in alternating (011) layers. Based on optical data, it has a band gap of 2.60 eV. Under UV irradiation, the Pt-modified semiconductor evolves small amounts of H_2 from aqueous methanol and very small amounts of O_2 from aqueous $AgNO_3$.[188] Bi_2WO_6 belongs to the $(Bi_2O_2)^{2+}$ $[A_{m-1}B_mO_{3m+1}]^{2-}$ Aurivillius structure type with alternating layers of corner-shared WO_6 and Bi_2O_2 layers (see Figure 2). $Bi_2W_2O_9$ is a defect structure, with the A sites remaining empty. After modification with Pt, it is slightly more active in an aqueous methanol solution than Bi_2WO_6 (UV irradiation). Under visible light, Bi_2WO_6 (2.8 eV) also catalyzes slow O_2 evolution from an aqueous $AgNO_3$ solution.[175] While the low-temperature (LT) modification of Bi_2MoO_6 (2.7 eV) is isomorphous with Bi_2WO_6 from above, the HT

form (3.02 eV) contains isolated Mo_4 tetrahedra (Figure 4).[189] Under UV and visible irradiation, both catalyze O_2 evolution from aqueous $AgNO_3$, with the LT form having higher activity than the HT form, presumably because of the lack of an efficient charge-transport pathway in the latter. No H_2 evolution from aqueous MeOH is observed for either material.[189] The structures (not shown) of $Bi_2Mo_2O_9$ (3.10 eV) and $Bi_2Mo_3O_{12}$ (2.88 eV) are similar to the HT form, and their activities for O_2 evolution from aqueous $AgNO_3$ are intermediate between the above materials.[189] The only other molybdates known to split water are $PbMoO_4$ and $Cr/PbMoO_4$.[190,191] Both crystallize in the Scheelite ($CaWO_4$) structure type, which contains WO_4 tetrahedra isolated by the Ca ions (Figure 4). Both have band gaps of 3.31 eV ($PbMoO_4$) and 2.16–2.43 eV ($Cr/PbMoO_4$), depending on the Cr content. $Pt/PbMoO_4$, but not any of the Cr-doped phases, evolves good rates of H_2 from an aqueous methanol solution under UV light. From pure water, O_2 evolution is fair, but no H_2 is formed. From aqueous $AgNO_3$, both the Cr-doped and pure phases evolve good rates of O_2,[190] with the performance of the Cr phases extended into the visible (>420 nm).[191] The band gap of CeO_2 (Fluorite structure, not shown) is between 2.79 and 3.18 eV, depending on the preparation. Under UV irradiation, CeO_2 catalyzes slow O_2 evolution from an aqueous $Fe_2(SO_4)_3$ solution.[185] When prepared by hydrolysis of CuCl, cuprous oxide Cu_2O (cuprite; ccp O lattice with Cu in ¼ of the T_d voids; structure not shown) evolves small but stoichiometric rates of H_2/O_2 under visible light irradiation from pure water. Cu_2O has a band gap of 2.0 eV (from UV/vis spectroscopy).[192] Later experiments showed that H_2/O_2 evolution is at least partially due to *mechanocatalysis*. This presently not understood process is driven by frictional energy released into the reaction mixture by stirring it with a stir bar.[193] Several binary metal oxides (Cu_2O, NiO, CO_3O_4, and Fe_3O_4) showed small activity for water splitting under mechanocatalytic conditions, while much lower, yet definite activity was also observed for RuO_2 and IrO_2. Cupric oxide (CuO) and Fe_2O_3 did not show activity for the reaction, and neither did TiO_2, ZnO, and WO_3.

Main-Group Metal Oxides

In very recent work, Inoue and co-workers demonstrated that the oxides of the main-group elements Ga, In, Ge, Sn, and Sb are effective photochemical water-splitting catalysts, although often only in the presence of suitable redox agents. In_2O_3 (2.7 eV) crystallizes in the $C-M_2O_3$ structure type (a defect Fluorite structure with ¼ of O removed, not shown).[66] After modification with a Pt cocatalyst, the material evolves small quantities of H_2/O_2 from aqueous solutions of methanol/$AgNO_3$, respectively, under visible light irradiation.[194] With NiO as a cocatalyst, small quantities of H_2 are formed from pure water (UV light). $Ba_2In_2O_5$ crystallizes in the Brownmillerite structure type consisting of alternating layers of corner-shared InO_4 tetrahedra and corner-shared InO_6 octahedra and Ba^{2+} ions between these units (Figure 4). Under visible irradiation, Pt-modified $Ba_2In_2O_5$ evolves small amounts of H_2/O_2 from aqueous solutions of methanol and $AgNO_3$, while NiO-modified $Ba_2In_2O_5$ evolves H_2 from pure water. Doping with Cr ions reduces the rates slightly, however, if the Cr-doped material is mixed with Cr/In_2O_3, the activity for H_2/O_2 evolution under visible light or UV is enhanced.[194] $In_2O_3(ZnO)_m$ ($m = 3$ and 9) crystallizes in a layered structure containing sheets of octahedral InO_6 units alternating with sheets of tetrahedral and trigonal-pyramidal ZnO_4 units (Figure 4).[195] The band gaps are 2.6/2.7 eV for $m = 3$ and 9, respectively. Under visible light irradiation, both materials evolve small quantities of H_2/O_2 from aqueous solutions of methanol and $AgNO_3$.[196] $CaIn_2O_4$ has a tetragonal crystal structure containing a network of edge-shared distorted InO_6 octahedra (Figure 4). Under UV irradiation, the RuO_2-modified semiconductor has some activity for overall water splitting, depending on the calcination temperature and RuO_2 loading. By comparison, the activities of RuO_2-modified $SrIn_2O_4$ (orthorhombic; Figure 4) and $LaInO_3$ are by factors of 3 and 10 lower.[197] While separate Ga_2O_3 and Lu_2O_3 evolve only traces of H_2 from aqueous methanol, the mixture of the two oxides forms an active (QE = 6.81% at 320 nm) water-splitting catalyst, after doping with Zn and modification with NiO particles.[198] The structure of β-Ga_2O_3 (Figure 4) consists of corner- and edge-shared GaO_6 octahedra and GaO_4 tetrahedra. Its absorption edge is 270 nm, suggesting a band gap of 4.6 eV. Lu_2O_3 crystallizes in the $C-M_2O_3$ structure type similar to In_2O_3 (see above). $ZnGa_2O_4$ is also known to catalyze the evolution of H_2 and O_2 from pure water under UV irradiation. After modification with RuO_2, H_2 and O_2 are evolved at near-stoichiometric but low rates. The catalyst activity strongly depends on the calcination temperature. The crystal structure of $ZnGa_2O_4$ (Figure 4) contains GaO_6 octahedra and ZnO_4 tetrahedra. The compound has a band gap of 4.3 eV from UV/vis spectra (2.78 eV from DFT calculations).[199] Sr_2SnO_4 can be viewed as a Ruddlesden–Popper phase with $m = 1$ (Figure 2). It is the only tin oxide known to split water photochemically, albeit at low rates, under UV irradiation, and only after modification with RuO_2.[200] For Sb, several oxides have been identified as water-splitting catalysts. After the addition of a RuO_2 cocatalyst, $M_2Sb_2O_7$ (M = Ca, Sr, Weberite), $CaSb_2O_6$, and $NaSbO_3$ (Ilmenite) all catalyze overall water splitting with near-stoichiometric O_2 evolution.[200,201] $NaSbO_3$ crystallizes in the Ilmenite structure containing layers of SbO_6 octahedra separated by Na ions (Figure 2). $M_2Sb_2O_7$ (M = Ca, Sr), on the other hand, crystallize in the Weberite structure type (Figure 4), containing corner-shared SbO_6 octahedra in two different environments. After modification with RuO_2, the activities remain generally low but increase in the order $CaSb_2O_6 < NaSbO_3 < Ca_2Sb_2O_7 < Sr_2Sb_2O_7$. This trend is correlated with the presence of increasingly distorted MO_6 octahedra in the more active structures.[201] Only traces of H_2/O_2 are evolved without a RuO_2 cocatalyst. In contrast to the alkaline-earth germanates (M_2GeO_4, M = Ca, Sr, Ba), Zn_2GeO_4 is stable under UV irradiation. Its Willemite structure (Figure 4) consists of a 3D network of corner-shared GeO_4 and ZnO_4 tetrahedra. Based on the absorption edge at 310 nm, the band gap is 4.0 eV. Under UV light, the RuO_2-modified catalyst evolves H_2 and O_2 in near-stoichiometric quantity from pure water.[202]

Metal Nitrides and Phosphides

In recent years, nitrides and nitride/oxide compounds of Ga and Ge have evolved as promising water-splitting catalysts that can operate under visible light and without external redox agents.[45,46] GaN:ZnO forms a solid solution in the Wurtzite structure type (not shown). Interestingly, the band gap of the solution (2.38 eV) is smaller than that of the separate components, GaN (3.4 eV) and ZnO (3.2 eV), which appears to be due to a raised valence band edge that results from p−d repulsion of Zn 3d and N 2p electrons. After modification with RuO_2, $Ga_{0.38}N_{0.33}Zn_{0.13}O_{0.16}$ splits water stoichiometrically into H_2 and O_2 at very good rates under UV and with reasonable rates under visible light (QE = 0.14% for 300–480 nm).[203,204] RuO_2 can be replaced with other cocatalysts (Rh, Ir, and Pt),[205] among which a mixed Cr/Rh oxide is the most effective (QE = 2.5%).[14,15] β-Ge_3N_4 crystallizes in the Phenacite structure type (see Figure 3), consisting of corner-shared GeN_4 tetrahedra. Despite its large band gap of 3.8–3.9 eV (absorption edge at 300 nm), the compound gives a broad luminescence at 480 nm (at 77 K). After modification with 20–50 nm RuO_2 particles, the semiconductor splits pure water stoichiometrically into H_2/O_2 with excellent activity under UV light (QE = 9%), while pure Ge_3N_4 is catalytically inactive.[206,207] Various Ga/Zn oxynitrides with band gaps of 2.66–4.31 eV can be obtained by doping $ZnGeN_2$ (wurtzite) with ZnO. Of these, the solid solution $Zn_{1.44}GeN_{2.08}O_{0.38}$ has a band gap of 2.7 eV. Upon modification with 1–5 wt % RuO_2 but not without it, the material catalyzes stoichiometric water splitting at medium rates. Under visible light, the activity is about 4 times lower.[208] Neither ZnO nor $ZnGeN_2$ split water under similar conditions. Ta_3N_5 crystallizes in the pseudo-Brookite structure (Figure 3) with edge- and corner-shared irregular TaN_6 octahedra. The O-doped form $Ta_3N_{4.8}O_{0.3}$ with a 2.1 eV band gap and a 600 nm absorption edge is obtained by the reaction of Ta_2O_5 with NH_3. After modification with Pt, this catalyst evolves very small rates of H_2 from aqueous MeOH under visible irradiation (QE = 0.1% at 420–600 nm). Prior calcination with La_2O_3 (buffers at pH = 8.5) leads to good rates of O_2 from aqueous $AgNO_3$, while without La_2O_3, N_2 is formed as a result of anodic dissolution of the catalyst under acidic conditions.[69,209] β-TaON is isomorphous with Baddeleyite, monoclinic ZrO_2 (Figure 4) and consists of edge-shared TaO_7 polyhedra. The reaction of Ta_2O_5 with NH_3 at 1123 K for 15 h affords a material with the composition $TaO_{1.24}N_{0.84}$,[210] whose band gap of 2.5 eV is estimated from a 500 nm absorption edge. Under visible light, the catalyst is quite active for O_2 evolution (QE = 34%) from aqueous $AgNO_3$, when La_2O_3 is added as a base buffer (pH = 8). With Pt, Rh, or Ir cocatalysts, the material evolves only small rates of H_2 from aqueous methanol (QE = 0.2%),[210] but with Ru, the activity increases significantly (QE = 0.8%).[44,211] Abe et al. found that, under visible light, TaON evolves small amounts of H_2 from an aqueous iodide solution.[187] In tandem with Pt−WO_3, stoichiometric water splitting is possible in the presence of iodide as a redox shuttle. The QE = 0.4% at 420 nm remained stable for up to 100 h.[187] The oxynitrides $MTaO_2N$ (M = Ca, Sr, Ba) all crystallize in the Perovskite structure type. The band gaps decrease with increasing the radius of the alkaline-earth metal: 2.5, 2.1, and 2.0 eV for M = Ca, Sr, and Ba, respectively. Under visible light, H_2 was formed from aqueous methanol, but no O_2 evolution took place, not even from aqueous $AgNO_3$.[44] $LaTiO_2N$ also has the Perovskite structure and a band gap of 2.1 eV. Under visible light, the Pt-modified catalyst slowly evolved H_2 from aqueous methanol (QE = 0.15%), and in the presence of $AgNO_3$ and La_2O_3 as a base buffer (pH = 8), O_2 is produced at reasonable rates during the first 10 h. The formation of N_2 can be suppressed by doping of the catalyst with La and by the addition of 2 wt % colloidal IrO_2 as a cocatalyst. Under optimized conditions, this catalyst evolves O_2 with QE = 5%.[212] $Y_2Ta_2O_5N_2$ crystallizes in the Pyrochlore structure type (Figure 3). The prepared $Y_2Ta_2O_{4.94}N_{2.18}$ is slightly nonstoichiometric and has an absorption edge of 560 nm, suggesting a band gap of 2.2 eV (compared to 3.8 nm for $YTaO_4$). Using visible light, the Pt/Ru-modified compound evolved good rates of H_2 from aqueous ethanol. The material containing separate Ru or Pt cocatalysts gave lower activity. Good O_2 evolution also occurred from aqueous $AgNO_3$ when La_2O_3 was added as a buffer. Only a small amount of N_2 was detected at the beginning of the reaction.[213] InP crystallizes in the zinc blende structure type (not shown) and has a band gap of 1.25 eV. With Pt as a cocatalyst, it evolves small quantities of H_2 from aqueous solutions containing sulfite and sulfide as electron donors when illuminated with UV light.[214] The catalytic nature of the process is doubtful.

Metal Sulfides

Metal sulfides are attractive as photochemical water-splitting catalysts because of their small band gaps that allow absorption of visible light. However, applications as catalysts have been hampered by the photochemical instability requiring the use of sacrificial donors for photochemical H_2 evolution from water. CdS (Wurtzite structure, not shown) is probably the best studied metal sulfide photocatalyst.[27,29,32,33] Because of its relatively narrow band gap (2.4 eV), it absorbs visible light at wavelengths of <510 nm. The flat-band potential of CdS (−0.87 V)[70] is sufficiently high to reduce H_2O, and the top of its valence band (1.5 V vs NHE) is theoretically suitable to allow oxidation of water. For 4 nm CdS nanoparticles, the lifetime of photogenerated charge carriers is on the order of 50 ps.[215] However, prolonged irradiation of CdS suspensions leads to photocorrosion of CdS into Cd^{2+} and S (sulfate in the presence of O_2).[71,216,217] This reaction can be suppressed by the addition of reducing agents to the aqueous phase (see below). Darwent and Porter[218,219] and separately Mills and Porter[93] were the first to investigate CdS for photochemical water splitting using EDTA as the sacrificial agent. Under visible light irradiation, Pt−CdS powder evolved H_2 from aqueous EDTA with QE = 4%, but without Pt, the activity was reduced by a factor of 10. Prolonged irradiation (>4 h) leads to decomposition of the catalyst.[93,219] In 1984, Reber and co-workers published the most comprehensive study on photocatalysis with CdS−Pt microcrystalline powders.[220] Among other variables, they studied the effect of various sacrificial electron donors and their concentrations, reaction temperature, pH, and of

irradiation wavelengths. The best catalysts evolved H_2 at 2.9 mmol/h/0.4 g (QE = 25%) under irradiation with light of >300 nm in the presence of either S^{2-}, SO_3^{2-}, or S^{2-}/HPO_2^- as reducing agents. The activity dropped by 21% over the course of 6 days, likely because of deactivitation of Pt due to formation of Pt-S species. Under solar irradiation, 50 mL/h of H_2 were produced with 0.4 g of catalyst suspension equal to an energy efficiency of 2%. In a follow-up study, the same team showed that the activity of CdS could be increased up to 357 mL/h/0.4 g (QE = 37%) of H_2 in aqueous Na_2S/Na_2SO_3 by doping CdS with 15 mol % ZnS and by the addition of a Pt cocatalyst.[217] The effect of Ag_2S coprecipitates, the specific surface area of the catalyst, and material decomposition were also tested. At about the same time, Gratzel's group published results on Pt−CdS−RuO_2 colloidal catalysts operating under visible light.[221] The CdS particles were synthesized in situ and identified via their absorption edge at 520 nm. Cofunctionalization with RuO_2 and Pt gave a catalyst that produced stoichiometric amounts of H_2/O_2 from pure water under visible light irradiation. The H_2 evolution increased with temperature. Without RuO_2, CdS was found to decompose rapidly with the formation of S. Similar results were obtained with CdS−Rh−RuO_2 and CdS−Pt–RuO_2 catalysts in a different laboratory.[222] In general, O_2 evolution from CdS-based catalysts is problematic.[21,70] To solve this problem and to address the photochemical instability of CdS, more recent studies have focused on other forms of CdS, including CdS nanoparticles stabilized in micelles,[223–225] CdS composites with other semiconductors (TiO_2,[226,227] ZnS,[228,229] and CdSe [230]), metal cocatalysts (Pt, Pd, Rh, Ru, Ir, Fe, Ni, and Co),[231,232] hollow CdS microparticles,[233] and Cu-doped CdS. [234,235] The effect of CdS preparation was also studied.[236,237] Despite these efforts, photocorrosion and the inability of water oxidation remain the principle problems of CdS-based water-splitting catalysts.

ZnS (zinc blende) is the other major metal sulfide investigated for photochemical water splitting. It has a band gap of 3.66 eV, which restricts light absorption to the UV (<340 nm). Similar to CdS, it undergoes photochemical decomposition into the components when irradiated in the absence of sacrificial electron donors.[13] The first report on water splitting with ZnS was published by Yamagida in 1983,[238] who synthesized ZnS from $Zn(SO_4)$ or $ZnCl_2$ and Na_2S in water. With tetrahydrofuran (THF) or alcohols as the sacrificial donor, this catalyst produced H_2 gas under UV irradiation. The addition of D_2O caused the production of D_2/H_2 with a ratio of 7, establishing water as the H_2 source. The most comprehensive study on photocatalysis of ZnS and ZnS−Pt was carried out by Reber et al.[13] The effect of catalyst preparation, sacrificial electron donors, pH, and temperature was investigated. Under irradiation with >300 nm light and at 60 °C, ZnS−Pt catalyzed H_2 evolution with quantum yields of up to 90% from aqueous solutions of sulfide and sulfite. Importantly, it was found that, in the presence of SO_3^{2-}, metallic Zn was formed, which was thought to assume a role in electron transfer to water. Long-time catalytic tests showed that no deactivation of ZnS occurred over 34 h. To improve visible light absorption of ZnS, Kudo's group has tested metal dopants (Cu, [239] Ni, [240] and Pb[241]). Doping can move the absorption edge to 500 nm in the case of Ni^{2+} ions and 550 nm in the case of Pb^{2+} ions. Under visible irradiation, a Ni^{2+}-doped catalyst produced H_2 from aqueous K_2SO_3/Na_2S with QEs of up to 1.3%.[240] Cu-doped ZnS gave QE = 3.7% under visible light irradiation from aqueous Na_2SO_3.[239] Doping of ZnS with variable amounts of $AgInS_2$ or $CuInS_2$ produces a series of solid solutions that crystallize in the cubic zinc blende or hexagonal Wurtzite structure.[242–245] The optical absorption of these materials can be adjusted between 400 and 800 nm, depending on the composition.[243] Visible light irradiation of the Pt- or Ru-derivatized catalysts produces H_2 with a QE of up to 7.5% from aqueous Na_2S/Ka_2SO_3.[243] For the Pt-loaded $Ag_{0.22}In_{0.22}Zn_{1.56}S_2$ photocatalyst, a QE of 20% was measured at 420 nm under solar irradiation conditions.[245]

While pure InS or In_2S_3 do not catalyze photochemical water splitting, several ternary indium sulfides do. $Na_5In_7S_{13}$ forms a Zeolite-like structure containing SIn_4 tetrahedral units (structure not shown) and has a band gap of 3.2 eV.[246] Under irradiation with a Xe lamp, the material evolves a fair rate of H_2 from a 0.5 M Na_2SO_3 aqueous solution. Using Na_2S as the sacrificial electron donor, $Na_{14}In_{17}Cu_3S_{35}\cdot xH_2O$ evolves small quantities of H_2 under visible light irradiation, equal to QE = 3.7% at 420 nm. With SO_3^{2-}, the QE drops to 0.37%. For $(AEP)_6In_{10}S_{18}$, AEP = protonated 1-(2-aminoethyl)piperazine, higher rates were observed.[247] The latter two compounds form complex networks of MS supertetrahedra (example in Figure 4). S and Zn doping of $In(OH)_3$ (ReO_3 structure, not shown) produces $[In(OH)_yS_z]$ and $In(OH)_yS_z$:Zn ($z \sim 2$) with absorption edges at 570 and 470 nm, respectively. Both catalysts evolve H_2 from aqueous sulfide/sulfite solutions under visible light illumination, with Pt-loaded Zn:$In(OH)_yS_z$ reaching QE = 0.59%.[248] $CuInS_2$ (zinc blende structure with Cu^+ and In^{3+} on tetrahedral sites, not shown) and $CuIn_5S_8$ (spinel structure; ccp lattice of S^{2-} with Cu^+ only in T_d voids and In^{3+} in both O_h and T_d voids) produce very low amounts of H_2 in the presence of sulfite and under UV light irradiation.[249] $NaInS_2$ has a layered structure consisting of layers of edge-shared octahedral InS_6 units (Figure 2). Its 2.3 eV band gap corresponds to an absorption edge of 550 nm. Under visible light irradiation, the Pt-modified catalyst showed good photocatalytic activity for H_2 evolution from an aqueous K_2SO_3 solution.[250] WS_2 forms the MoS_2 structure (not shown) containing layers of trigonal-prismatic WS_6 units. It has a 1.7 eV direct band gap and a 1.3 eV indirect band gap. When supported on SiO_2 and using fluoresceine as a sensitizer, the catalyst produced H_2 from aqueous EDTA solutions under visible light.[251] Bi_2S_3 crystallizes in the Bismuthinite structure type containing chains of corner-shared BiS_4 tetrahedra (Figure 4). It has a band gap of 1.28 eV. Under visible irradiation, it produces H_2 at intermediate rates from an aqueous sulfide solution. Rates decline after 100 min, probably because of disulfide formation. Platinization improves the activity by 25%.[252] Other metal sulfides have also been tested.[234] Of these, In_2Se_3, SnS_2, HgS, Tl_2S,PdS, EuS, CuS, FeS, CoS, and Fe_2S_3 were found to be inactive because of their small band gaps (<2 eV).

Summary

1. Only metal compounds with d^0 ions (Ti, Zr, Nb, and Ta) and d^{10} ions (Ga, In, Ge, Sn, and Sb) have activity for *overall* photochemical splitting of water. Oxides are dominant, but nitrides and oxynitrides (GaN:ZnO and Ge_3N_4) are also known to catalyze the reaction.

2. Other catalysts require reducing agents (alcohols, sulfides, sulfites, and EDTA) or oxidizing agents (persulfate and Ce^{4+} or Ag^+ ions) to facilitate either water reduction or oxidation. An overall water splitting might be achievable with these materials by coupling of appropriate semiconductor pairs into tandem systems according to Figure 1D (for examples, see refs 107, 108, 118, and 187).

3. Semiconductors containing metal ions with partially filled orbitals generally show reduced or no catalytic activity, because the ions act as catalytic centers for electron–hole recombination.[48,124,190,191,194] Exceptions are diamagnetic ions with the d^{10} configuration (Ag^+, Zn^{2+}, and Cu^+), as seen in various semiconductors (Table 1), and ions with s^2 configuration (Pb^{2+} and Bi^{3+}), as in $PbTiO_3$ and $PbBi_4Ti_4O_{15}$,[127] $PbBi_2Nb_2O_9$,[113] $PbMoO_4$,[190] and Pb:ZnS.[241] The fact that electron–hole recombination seems to be less dominant for Ni^{2+} ions (e.g., in Ni:InO_4,[47,62] $NiTa_2O_6$,[48] and Ni:ZnS,[240]) has been attributed to the difficulty of accessing 1+/3+ oxidation states for this ion.[48]

4. All metal sulfides, including CdS and ZnS, undergo photochemical decomposition in the absence of sacrificial electron donors.[13,93,219]

5. The only visible-light-driven catalysts that split water and do not require external redox agents are NiO/RuO_2−Ni:$InTaO_4$ (QE = 0.66%),[47,62] the Pt−WO_3 and Pt/$SrTiO_3$:TaON (QE = 0.1%) tandem system,[118,186,187] Cr/Rh−GaN:ZnO (QE = 2.5%),[14,15,205] and $(Zn_{1.44}Ge)(N_{2.08}O_{0.38})$ (QE not determined).[208]

6. Trends in H_2/O_2 evolution rates roughly follow the size of the semiconductor *band gaps*. Group 13/14 element oxides (2.7–3.8 eV) are generally less active than titanates (TiO_2, 3.0–3.1 eV). Niobates (Nb_2O_5, 3.1–3.5 eV) are more active than titanates but less active than tantalates (Ta_2O_5, 4.0–4.6 eV). Here, larger bandgaps reflect an increasing thermodynamic driving force for water splitting. The low activity of ZrO_2 in spite of its large band gap (5.0–5.7 eV) may be explained with poor spectral overlap of its absorption (<217–248 nm) with commonly used Xe and Hg light sources. The low activity of Sr_2SnO_4 (3.8 eV) is likely a result of the low flat-band potential, which is ineffective for proton reduction.

7. Activities strongly depend on *cocatalysts*. In the majority of cases, cocatalysts enable (e.g., Ta_2O_5) [40,48] or increase the water-splitting activity of a semiconductor. Many semiconductors evolve H_2 from water but O_2 only in the presence of a cocatalyst (often NiO). This behavior is likely due to the greater complexity of O_2 evolution (a four-electron process) compared to H_2 (a two-electron process). Very few semiconductors experience a decrease in activity upon attachment of a cocatalyst. For example, ZrO_2 is more active without Pt, Cu, Au, or RuO_2 cocatalysts,[137] as is the Ruddlesden–Popper phase $H_2SrTa_2O_7$.[144] These observations may be explained with the large band gaps of these semiconductors and possible electron–hole recombination on the metal cocatalyst. In other cases, low activities are caused by back-reaction of H_2 and O_2 (the reverse of reaction 1), a problem particularly relevant for Pt.[95] Au particles do not promote this back-reaction but catalyze the reduction of O_2 in competition with H_2O.[97] For many catalysts, the activity is strongly dependent on the cocatalyst material (see, for example, $K_2La_2Ti_3O_{10}$[132,133] and GaN:ZnO[14,15,203–205]) and on the methods of cocatalyst attachment (see $SrTiO_3$,[117] $Cs_2Nb_4O_{11}$,[180] and CdS[220]). These dependencies must be attributed to variations in charge transport across the cocatalyst−semiconductor interface.

8. *Additives* (other than sacrificial redox agents) often enhance the activity of the catalyst. Base buffers, like La_2O_3, can stabilize sensitive metal nitrides against photochemical decomposition.[44,69,209,211] For TiO_2 and other metal oxides, metal hydroxides and carbonates can suppress the readsorption of O_2 as superperoxide or peroxide.[29,40,41,93–96,137]

9. The *crystal structure* of a semiconductor can have a marked influence on the catalytic activity. Active catalysts are generally found to have efficient charge-transport pathways that connect the interior with the surface where water splitting occurs.[123,156,157,189] Oxide-bridged metal ions that can assume such a role are present in the majority of structures discussed in this review. The structures of $LaNbO_4$, $BiVO_4$ (both Fergusonite), $CaWO_4$ (Scheelite), and HT Bi_2MoO_6 contain isolated metal oxide polyhedra, and as a consequence, their catalytic activities are low. Other authors have correlated distortions in metal oxide polyhedra with the catalytic activity. In the case of RuO_2-modified $BaTi_4O_9$, for example, distorted TiO_6 octahedra are believed to cause dipole moments that aid electron–hole separation.[42] Similar arguments were used for the series $M_2Ti_6O_{13}$ (M = Na, K, Rb)[42,135] and for $M_2Sb_2O_7$ (M = Ca, Sr, Weberite), $CaSb_2O_6$, and $NaSbO_3$ (Ilmenite).[200,201] For $KTaO_3$, the cation size of the Ti, Zr, and Hf dopants could be correlated with the distortion of the structure and the O_2 production rate and inversely with the H_2 production rate.[145] Cavities in the structures of the so-called tunnel titanates $M_2Ti_6O_{13}$ (M = Na, K, Rb)[42,135] have also been implicated in enhanced electrical contact to the RuO_2 cocatalyst. Because of their small size (~1 nm), the cocatalyst particles are believed to fit well into the opening of the tunnels. Finally, the high activities of some of the layered Perovskites are attributed to the incorporation of water into the interlayer space.[43,169] Water incorporation increases the interfacial area and reduces the necessary distance for charge transfer.

10. Effects of *crystal morphology* and *specific surface area*. Because of their physical relationship, these two variables cannot be separately discussed. In general, an increase in the specific surface area (i.e., a reduction in the crystal size) leads to higher catalytic activities. For example, see $La_2Ti_2O_7$,[125] $Sr_3Ti_2O_7$,[126] $K_2La_2Ti_3O_{10}$,[134] $NaTaO_3$,[143] $KCa_2Nb_3O_{10}$,[172] NiO-La:$NaTaO_3$,[12] and $Ba_5Nb_4O_{15}$.[181] The same applies to the layered Perovskites, which have the ability to increase their interfacial area by incorporating water into the interlayer space (see point. 9 above).[169] Finally, there are also cases where the surface area does not matter (e.g., ZnS)[13] or where the activity diminishes with an increase in the surface area (CdS and ZnS).[13,217] The reasons for the latter behavior are not clear.

In conclusion, over 130 semiconductors are known to catalyze the photochemical water-splitting reaction according to eq 1 or either water oxidation or reduction in the presence of sacrificial agents. Even though the principle activity-controlling factors in semiconductor-heterostructures have been identified, many aspects of the function of inorganic photocatalysts are still unclear. Most importantly, the molecular mechanism of water reduction and oxidation on the semiconductor surface has not yet been elucidated in sufficient detail.[78,98,100,102,103,106] Many questions about charge transfer between semiconductor and cocatalysts, and its dependence on the structural and electronic features of the interface are still open.[253–257] The effect of variable material preparations and surface impurities on the catalytic activity of semiconductors (e.g. sulfur and oxide on CdS[70,71,220]) have not been fully considered. These areas represent significant opportunities for improving water splitting photocatalysts. The development of better catalysts is also going to benefit from recent progress in nanoscience. Quantum size effects can now be used for tailoring both electronic structure and reactivity of nanostructures,[99,258] and synthetic methods can be employed for controlling the morphology of catalysts down to the nanoscale. In combination with modern analytical techniques (e.g. scanning transmission electron microscopy) for materials characterization, these advances will help to further raise the efficiency of photochemical water splitting catalysts.

Acknowledgment. This work was supported by the Energy Innovations Small Grant program of the California Energy Commission.

References

(1) Lewis, N. S.; Nocera, D. G. *Proc. Natl. Acad. Sci. U.S.A.* **2006**, *103* (43), 15729–15735.
(2) Lewis, N. S.; Crabtree, G.; Nozik, A. J.; Wasielewski, M. R.; Alivisatos, A. P. *Basic Research Needs for Solar Energy Utilization*; U.S. Department of Energy: Washington, DC, 2005.
(3) Huynh, W. U.; Dittmer, J. J.; Alivisatos, A. P. *Science* **2002**, *295* (5564), 2425–2427.
(4) Bach, U.; Lupo, D.; Comte, P.; Moser, J. E.; Weissortel, F.; Salbeck, J.; Spreitzer, H.; Gratzel, M. *Nature* **1998**, *395* (6702), 583–585.
(5) Gratzel, M. *Nature* **2001**, *414* (6861), 338–344.
(6) Green, M. A. Emery, K.; King, D. L.; Igari, S.; Warta, W. *Prog. Photovoltaics* **2005**, *13* (5), 387–392.
(7) Frank, A. J.; Kopidakis, N.; van de Lagemaat, J. *Coord. Chem. Rev.* **2004**, *248* (13–14), 1165–1179.
(8) Heller, A. *Acc. Chem. Res.* **1981**, *14* (5), 154–162.
(9) Law, M.; Greene, L. E.; Johnson, J. C.; Saykally, R.; Yang, P. D. *Nat. Mater.* **2005**, *4* (6), 455–459.
(10) Fujishima, A.; Honda, K. *Nature* **1972**, *238* (5358), 37.
(11) Fujishima, A.; Honda, K. *B. Chem. Soc. Jpn.* **1971**, *44* (4), 1148.
(12) Kato, H.; Asakura, K.; Kudo, A. *J. Am. Chem. Soc.* **2003**, *125* (10), 3082–3089.
(13) Reber, J. F.; Meier, K. *J. Phys. Chem.* **1984**, *88* (24), 5903–5913.
(14) Maeda, K.; Teramura, K.; Lu, D. L.; Takata, T.; Saito, N.; Inoue, Y.; Domen, K. *J. Phys. Chem. B* **2006**, *110* (28), 13753–13758.
(15) Maeda, K.; Teramura, K.; Lu, D. L.; Takata, T.; Saito, N.; Inoue, Y.; Domen, K. *Nature* **2006**, *440* (7082), 295–295.
(16) Nowotny, J.; Sorrell, C. C.; Bak, T.; Sheppard, L. R. *Sol. Energy* **2005**, *78* (5), 593–602.
(17) Turner, J. A. *Science* **1999**, *285* (5433), 1493–1493.
(18) Bak, T. Nowotny, J.; Rekas, M.; Sorrell, C. C. *Int. J. Hydrogen Energy* **2002**, *27* (10), 991–1022.
(19) Kamat, P. V.; Meisel, D. *Compt. Rend. Chim.* **2003**, *6* (8–10), 999–1007.
(20) Levy, B. *J. Electroceram.* **1997**, *1* (3), 239–272.
(21) Mills, A.; LeHunte, S. *J. Photochem. Photobiol. A* **1997**, *108* (1), 1–35.
(22) Harriman, A.; Pickering, I. J.; Thomas, J. M.; Christensen, P. A. *J. Chem. Soc., Faraday Trans. 1* **1988**, *84*, 2795–2806.
(23) Mills, A.; Russell, T. *J. Chem. Soc., Faraday Trans.* **1991**, *87* (8), 1245–1250.
(24) McEvoy, J. P.; Brudvig, G. W. *Chem. Rev.* **2006**, *106* (11), 4455–4483.
(25) Yagi, M.; Kaneko, M. *Chem. Rev.* **2001**, *101* (1), 21–35.
(26) Alstrum-Acevedo, J. H.; Brennaman, M. K.; Meyer, T. J. *Inorg. Chem.* **2005**, *44* (20), 6802–6827.
(27) (a) Kamat, P. V.; Dimitrijevic, N. M. *Sol. Energy* **1990**, *44* (2), 83–98. (b) Kamat, P. V. *J. Phys. Chem. C* **2007**, *111*, 2834–2860.
(28) Henglein, A. *Top. Curr. Chem.* **1988**, *143*, 113–180.
(29) Gratzel, M. *Acc. Chem. Res.* **1981**, *14* (12), 376–384.
(30) Kiwi, J.; Kalyanasundaram, K.; Gratzel, M. *Struct. Bonding (Berlin)* **1982**, *49*, 37–125.
(31) Gratzel, M. *Faraday Discuss.* **1980**, (70), 359–374.
(32) Kalyanasundaram, K.; Gratzel, M.; Pelizzetti, E. *Coord. Chem. Rev.* **1986**, *69*, 57–125.
(33) Ashokkumar, M. *Int. J. Hydrogen Energy* **1998**, *23* (6), 427–438.
(34) Kudo, A. *Catal. Surv. Asia* **2003**, *7* (1), 31–38.
(35) Moon, S. C.; Matsumura, Y.; Kitano, M.; Matsuoka, M.; Anpo, M. *Res. Chem. Intermed.* **2003**, *29* (3), 233–256.
(36) Li, D. F.; Zheng, J.; Chen, X. Y.; Zou, Z. G. *Prog. Chem.* **2007**, *19* (4), 464–477.
(37) Kudo, A.; Kato, H.; Tsuji, I. *Chem. Lett.* **2004**, *33* (12), 1534–1539.
(38) Takata, T.; Tanaka, A.; Hara, M.; Kondo, J. N.; Domen, K. *Catal. Today* **1998**, *44* (1–4), 17–26.
(39) Kudo, A. *Int. J. Hydrogen Energy* **2006**, *31* (2), 197–202.
(40) Sayama, K.; Arakawa, H. *J. Photochem. Photobiol. A* **1994**, *77* (2–3), 243–247.
(41) Arakawa, H. Water Photolysis by TiO_2 Particles—Significant Effect of Na_2CO_3 Addition on Water Splitting. In *Photocatalysis Science and Technology*; Kaneko, M., Okura, I., Eds.; Springer: New York, 2002; pp 235–248.
(42) Inoue, Y. Water Photolysis by Titanates with Tunnel Structures. In *Photocatalysis Science and Technology*; Kaneko, M., Okura, I., Eds.; Springer: New York, 2002; pp 249–260.
(43) Domen, K. Water Photolysis by Layered Compounds. In *Photocatalysis Science and Technology*; Kaneko, M., Okura, I., Eds.; Springer: New York, 2002; pp 261–278.
(44) Yamasita, D.; Takata, T.; Hara, M.; Kondo, J. N.; Domen, K. *Solid State Ionics* **2004**, *172* (1–4), 591–595.
(45) Maeda, K.; Teramura, K.; Saito, N.; Inoue, Y.; Kobayashi, H.; Domen, K. *Pure Appl. Chem.* **2006**, *78* (12), 2267–2276.
(46) Maeda, K.; Domen, K. *J. Phys. Chem. C* **2007**, *111* (22), 7851–7861.
(47) Zou, Z. G.; Arakawa, H. *J. Photochem. Photobiol. A* **2003**, *158* (2–3), 145–162.
(48) Kato, H.; Kudo, A. *Chem. Phys. Lett.* **1998**, *295* (5–6), 487–492.
(49) Shangguan, W. F. *Sci. Technol. Adv. Mater.* **2007**, *8* (1–2), 76–81.
(50) Maruska, H. P.; Ghosh, A. K. *Sol. Energy* **1978**, *20* (6), 443–458.
(51) Bard, A. J. *Science* **1980**, *207* (4427), 139–144.
(52) Bard, A. J.; Fox, M. A. *Acc. Chem. Res.* **1995**, *28* (3), 141–145.
(53) Gratzel, M. *Chem. Lett.* **2005**, *34* (1), 8–13.
(54) Bard, A. J. *J. Phys. Chem.* **1982**, *86* (2), 172–177.
(55) Nozik, A. J.; Memming, R. *J. Phys. Chem.* **1996**, *100* (31), 13061–13078.
(56) Tan, M. X.; Laibinis, P. E.; Nguyen, S. T.; Kesselman, J. M.; Stanton, C. E.; Lewis, N. S. Principles and Applications of Semiconductor Photoelectrochemistry. *Progress in Inorganic Chemistry*; John Wiley & Sons: New York, 1994; Vol. 41, pp 21–144.
(57) Memming, R. *Top. Curr. Chem.* **1988**, *143*, 79–112.
(58) Nozik, A. J. *Annu. Rev. Phys. Chem.* **1978**, *29*, 189–222.
(59) Bolton, J. R.; Strickler, S. J.; Connolly, J. S. *Nature* **1985**, *316* (6028), 495–500.
(60) Pleskov, Y. Y.; Gurevich, Y. V. *Semiconductor Photoelectrochemistry*; Consultants Bureau: New York, 1986; p 422.
(61) Rajeshwar, K. *J. Appl. Electrochem.* **2007**, *37* (7), 765–787.
(62) Zou, Z. G.; Ye, J. H.; Sayama, K.; Arakawa, H. *Nature* **2001**, *414* (6864), 625–627.
(63) Vogel, R.; Hoyer, P.; Weller, H. *J. Phys. Chem.* **1994**, *98* (12), 3183–3188.
(64) Fujishima, A.; Narasinga Rao, T. Photoelectrochemical Processes of Semiconductors. In *Photocatalysis Science and Technology*; Kaneko, M., Okura, I., Eds.; Springer: New York, 2002; pp 9–28.
(65) Nakato, Y. Photoelectrochemistry at Semiconductor/Liquid Interfaces. In *Photocatalysis Science and Technology*; Kaneko, M., Okura, I., Eds.; Springer: New York, 2002; pp 51–68.
(66) Fujii, M.; Kawai, T.; Kawai, S. *Chem. Phys. Lett.* **1984**, *106* (6), 517–522.
(67) Rajeshwar, K.; de Tacconi, N. R.; Chenthamarakshan, C. R. *Chem. Mater.* **2001**, *13* (9), 2765–2782.
(68) Kung, H. H.; Jarrett, H. S.; Sleight, A. W.; Ferretti, A. *J. Appl. Phys.* **1977**, *48* (6), 2463–2469.
(69) Chun, W. J.; Ishikawa, A.; Fujisawa, H.; Takata, T.; Kondo, J. N.; Hara, M.; Kawai, M.; Matsumoto, Y.; Domen, K. *J. Phys. Chem. B* **2003**, *107* (8), 1798–1803.
(70) Meissner, D.; Memming, R.; Kastening, B. *J. Phys. Chem.* **1988**, *92* (12), 3476–3483.
(71) Meissner, D.; Memming, R.; Kastening, B.; Bahnemann, D. *Chem. Phys. Lett.* **1986**, *127* (5), 419–423.
(72) Gurevich, Y. Y.; Pleskov, Y. V. *Semiconductor Photoelectrochemistry*; Consultants Bureau: New York, 1986; p 422.
(73) Butler, M. A.; Ginley, D. S. *J. Electrochem. Soc.* **1978**, *125* (2), 228–232.
(74) Kim, Y. I.; Atherton, S. J.; Brigham, E. S.; Mallouk, T. E. *J. Phys. Chem.* **1993**, *97* (45), 11802–11810.

(75) Kuhn, H. J.; Braslavsky, S. E.; Schmidt, R. *Pure Appl. Chem.* **2004**, *76* (12), 2105–2146.
(76) Ni, M.; Leung, M. K. H.; Leung, D. Y. C.; Sumathy, K. *Renewable Sustainable Energy Rev.* **2007**, *11* (3), 401–425.
(77) Anpo, M.; Dohshi, S.; Kitano, M.; Hu, Y.; Takeuchi, M.; Matsuoka, M. *Annu. Rev. Mater. Res.* **2005**, *35*, 1–27.
(78) Thompson, T. L.; Yates, J. T. *Chem. Rev.* **2006**, *106* (10), 4428–4453.
(79) Wrighton, M. S.; Ginley, D. S.; Wolczanski, P. T.; Ellis, A. B.; Morse, D. L.; Linz, A. *Proc. Natl. Acad. Sci. U.S.A.* **1975**, *72* (4), 1518–1522.
(80) Schrauzer, G. N.; Guth, T. D. *J. Am. Chem. Soc.* **1977**, *99* (22), 7189–7193.
(81) Van Damme, H.; Hall, W. K. *J. Am. Chem. Soc.* **1979**, *101* (15), 4373–4374.
(82) Kawai, T.; Sakata, T. *Chem. Phys. Lett.* **1980**, *72* (1), 87–89.
(83) Nozik, A. J. *Appl. Phys. Lett.* **1977**, *30* (11), 567–569.
(84) Durr, H.; Bossmann, S.; Beuerlein, A. *J. Photochem. Photobiol. A* **1993**, *73* (3), 233–245.
(85) Sato, S.; White, J. M. *Chem. Phys. Lett.* **1980**, *72* (1), 83–86.
(86) Kalyanasundaram, K.; Gratzel, M. *Angew. Chem., Int. Ed. Engl.* **1979**, *18* (9), 701–702.
(87) Kiwi, J.; Gratzel, M. *Angew. Chem., Int. Ed. Engl.* **1979**, *18* (8), 624–626.
(88) Kiwi, J.; Gratzel, M. *Nature* **1979**, *281* (5733), 657–658.
(89) Kiwi, J.; Borgarello, E.; Pelizzetti, E.; Visca, M.; Gratzel, M. *Angew. Chem., Int. Ed. Engl.* **1980**, *19* (8), 646–648.
(90) Borgarello, E.; Kiwi, J.; Pelizzetti, E.; Visca, M.; Gratzel, M. *J. Am. Chem. Soc.* **1981**, *103* (21), 6324–6329.
(91) Duonghong, D.; Borgarello, E.; Gratzel, M. *J. Am. Chem. Soc.* **1981**, *103* (16), 4685–4690.
(92) Borgarello, E.; Kiwi, J.; Pelizzetti, E.; Visca, M.; Gratzel, M. *Nature* **1981**, *289* (5794), 158–160.
(93) Mills, A.; Porter, G. *J. Chem. Soc., Faraday Trans. 1* **1982**, *78*, 3659–3669.
(94) Kiwi, J.; Gratzel, M. *J. Phys. Chem.* **1984**, *88* (7), 1302–1307.
(95) Yamaguti, K.; Sato, S. *J. Chem. Soc., Faraday Trans. 1* **1985**, *81*, 1237–1246.
(96) Sayama, K.; Arakawa, H. *J. Chem. Soc., Chem. Commun.* **1992**, (2), 150–152.
(97) Iwase, A.; Kato, H.; Kudo, A. *Catal. Lett.* **2006**, *108* (1–2), 6–9.
(98) Linsebigler, A. L.; Lu, G. Q.; Yates, J. T. *Chem. Rev.* **1995**, *95* (3), 735–758.
(99) Subramanian, V.; Wolf, E. E.; Kamat, P. V. *J. Am. Chem. Soc.* **2004**, *126* (15), 4943–4950.
(100) Yoshihara, T.; Katoh, R.; Furube, A.; Tamaki, Y.; Murai, M.; Hara, K.; Murata, S.; Arakawa, H.; Tachiya, M. *J. Phys. Chem. B* **2004**, *108* (12), 3817–3823.
(101) Ramakrishna, G.; Singh, A. K.; Palit, D. K.; Ghosh, H. N. *J. Phys. Chem. B* **2004**, *108* (5), 1701–1707.
(102) Yamakata, A.; Ishibashi, T.; Onishi, H. *J. Mol. Catal. A: Chem.* **2003**, *199* (1–2), 85–94.
(103) Kolle, U.; Moser, J.; Gratzel, M. *Inorg. Chem.* **1985**, *24* (14), 2253–2258.
(104) Bahnemann, D.; Henglein, A.; Lilie, J.; Spanhel, L. *J. Phys. Chem.* **1984**, *88* (4), 709–711.
(105) Rothenberger, G.; Moser, J.; Gratzel, M.; Serpone, N.; Sharma, D. K. *J. Am. Chem. Soc.* **1985**, *107* (26), 8054–8059.
(106) Gravelle, P. C.; Meriaude., P.; Teichner, S. J.; Juillet, F. *Discuss. Faraday Soc.* **1971**, (52), 140–&–8059.
(107) Abe, R.; Sayama, K.; Domen, K.; Arakawa, H. *Chem. Phys. Lett.* **2001**, *344* (3–4), 339–344.
(108) Abe, R.; Sayama, K.; Sugihara, H. *J. Phys. Chem. B* **2005**, *109* (33), 16052–16061.
(109) Sakthivel, S.; Kisch, H. *Angew. Chem., Int. Ed.* **2003**, *42* (40), 4908–4911.
(110) Asahi, R.; Morikawa, T.; Ohwaki, T.; Aoki, K.; Taga, Y. *Science* **2001**, *293* (5528), 269–271.
(111) Sakthivel, S.; Kisch, H. *ChemPhysChem* **2003**, *4* (5), 487–490.
(112) Ohno, T.; Mitsui, T.; Matsumura, M. *Chem. Lett.* **2003**, *32* (4), 364–365.
(113) Kim, H. G.; Hwang, D. W.; Lee, J. S. *J. Am. Chem. Soc.* **2004**, *126* (29), 8912–8913.
(114) Wrighton, M. S.; Ellis, A. B.; Wolczanski, P. T.; Morse, D. L.; Abrahamson, H. B.; Ginley, D. S. *J. Am. Chem. Soc.* **1976**, *98* (10), 2774–2779.
(115) Ohashi, K.; McCann, J.; Bockris, J. O. M. *Nature* **1977**, *266* (5603), 610–611.
(116) Domen, K.; Naito, S.; Soma, M.; Onishi, T.; Tamaru, K. *J. Chem. Soc., Chem. Commun.* **1980**, (12), 543–544.
(117) Domen, K.; Naito, S.; Onishi, T.; Tamaru, K. *Chem. Phys. Lett.* **1982**, *92* (4), 433–434.
(118) Sayama, K.; Mukasa, K.; Abe, R.; Abe, Y.; Arakawa, H. *Chem. Commun.* **2001**, (23), 2416–2417.
(119) Lehn, J. M.; Sauvage, J. P.; Ziessel, R. *Nouv. J. Chim.* **1980**, *4* (11), 623–627.
(120) Lehn, J. M.; Sauvage, J. P.; Ziessel, R.; Hilaire, L. *Isr. J. Chem.* **1982**, *22* (2), 168–172.
(121) Kim, J.; Hwang, D. W.; Kim, H. G.; Bae, S. W.; Lee, J. S.; Li, W.; Oh, S. H. *Top. Catal.* **2005**, *35* (3–4), 295–303.
(122) Kim, H. G.; Hwang, D. W.; Kim, J.; Kim, Y. G.; Lee, J. S. *Chem. Commun.* **1999**, (12), 1077–1078.
(123) Abe, R.; Higashi, M.; Sayama, K.; Abe, Y.; Sugihara, H. *J. Phys. Chem. B* **2006**, *110* (5), 2219–2226.
(124) Hwang, D. W.; Kirn, H. G.; Lee, J. S.; Kim, J.; Li, W.; Oh, S. H. *J. Phys. Chem. B* **2005**, *109* (6), 2093–2102.
(125) Song, H.; Cai, P.; Huabing, Y.; Yan, C. *Catal. Lett.* **2007**, *113* (1–2), 54–58.
(126) Jeong, H.; Kim, T.; Kim, D.; Kim, K. *Int. J. Hydrogen Energy* **2006**, *31* (9), 1142–1146.
(127) Kim, H. G.; Becker, O. S.; Jang, J. S.; Ji, S. M.; Borse, P. H.; Lee, J. S. *J. Solid State Chem.* **2006**, *179* (4), 1214–1218.
(128) Ishikawa, A.; Takata, T.; Kondo, J. N.; Hara, M.; Kobayashi, H.; Domen, K. *J. Am. Chem. Soc.* **2002**, *124* (45), 13547–13553.
(129) Takata, T.; Furumi, Y.; Shinohara, K.; Tanaka, A.; Hara, M.; Kondo, J. N.; Domen, K. *Chem. Mater.* **1997**, *9* (5), 1063.
(130) Gopalakrishnan, J.; Bhat, V. *Inorg. Chem.* **1987**, *26* (26), 4299–4301.
(131) Kudo, A.; Sakata, T. *J. Phys. Chem.* **1995**, *99* (43), 15963–15967.
(132) Tai, Y. W.; Chen, J. S.; Yang, C. C.; Wan, B. Z. *Catal. Today* **2004**, *97* (2–3), 95–101.
(133) Takata, T.; Shinohara, K.; Tanaka, A.; Hara, M.; Kondo, J. N.; Domen, K. *J. Photochem. Photobiol. A* **1997**, *106* (1–3), 45–49.
(134) Ikeda, S.; Hara, M.; Kondo, J. N.; Domen, K.; Takahashi, H.; Okubo, T.; Kakihana, M. *Chem. Mater.* **1998**, *10* (1), 72–77.
(135) Ogura, S.; Kohno, M.; Sato, K.; Inoue, Y. *Appl. Surf. Sci.* **1997**, *121*, 521–524.
(136) Kapoor, M. P.; Inagaki, S.; Yoshida, H. *J. Phys. Chem. B* **2005**, *109* (19), 9231–9238.
(137) Sayama, K.; Arakawa, H. *J. Phys. Chem.* **1993**, *97* (3), 531–533.
(138) Chang, S. M.; Doong, R. A. *J. Phys. Chem. B* **2004**, *108* (46), 18098–18103.
(139) Fukumoto, A.; Miwa, K. *Phys. Rev. B* **1997**, *55* (17), 11155–11160.
(140) Sayama, K.; Arakawa, H.; Domen, K. *Catal. Today* **1996**, *28* (1–2), 175–182.
(141) Kato, H.; Kudo, A. *Catal. Lett.* **1999**, *58* (2–3), 153–155.
(142) Kato, H.; Kudo, A. *J. Phys. Chem. B* **2001**, *105* (19), 4285–4292.
(143) Lin, W. H.; Cheng, C.; Hu, C. C.; Teng, H. S. *Appl. Phys. Lett.* **2006**, *89* (21), 211904211904–3.
(144) Shimizu, K.; Itoh, S.; Hatamachi, T.; Kodama, T.; Sato, M.; Toda, K. *Chem. Mater.* **2005**, *17* (20), 5161–5166.
(145) Mitsui, C.; Nishiguchi, H.; Fukamachi, K.; Ishihara, T.; Takita, Y. *Chem. Lett.* **1999**, (12), 1327–1328.
(146) Hagiwara, H.; Ono, N.; Inoue, T.; Matsumoto, H.; Ishihara, T. *Angew. Chem., Int. Ed.* **2006**, *45* (9), 1420–1422.
(147) Kato, H.; Kudo, A. *Chem. Lett.* **1999**, (11), 1207–1208.
(148) Ikeda, S.; Fubuki, M.; Takahara, Y. K.; Matsumura, M. *Appl. Catal. A* **2006**, *300* (2), 186–190.
(149) Yoshioka, K.; Petrykin, V.; Kakihana, M.; Kato, H.; Kudo, A. *J. Catal.* **2005**, *232* (1), 102–107.
(150) Luan, J. F.; Hao, X. P.; Zheng, S. R.; Luan, G. Y.; Wu, X. S. *J. Mater. Sci.* **2006**, *41* (23), 8001–8012.
(151) Kudo, A.; Kato, H.; Nakagawa, S. *J. Phys. Chem. B* **2000**, *104* (3), 571–575.
(152) Yao, W. F.; Ye, J. H. *Chem. Phys. Lett.* **2007**, *435* (1–3), 96–99.
(153) Otsuka, H.; Kim, K. Y.; Kouzu, A.; Takimoto, I.; Fujimori, H.; Sakata, Y.; Imamura, H.; Matsumoto, T.; Toda, K. *Chem. Lett.* **2005**, *34* (6), 822–823.
(154) Kudo, A.; Kato, H. *Chem. Lett.* **1997**, (9), 867–868.
(155) Kurihara, T.; Okutomi, H.; Miseki, Y.; Kato, H.; Kudo, A. *Chem. Lett.* **2006**, *35* (3), 274–275.
(156) Abe, R.; Higashi, M.; Zou, Z. G.; Sayama, K.; Abe, Y.; Arakawa, H. *J. Phys. Chem. B* **2004**, *108* (3), 811–814.
(157) Machida, M.; Murakami, S.; Kijima, T.; Matsushima, S.; Arai, M. *J. Phys. Chem. B* **2001**, *105* (16), 3289–3294.
(158) Machida, M.; Yabunaka, J.; Kijima, T. *Chem. Mater.* **2000**, *12* (3), 812–817.
(159) Machida, M.; Yabunaka, J.; Kijima, T. *Chem. Commun.* **1999**, (19), 1939–1940.
(160) Domen, K.; Kudo, A.; Shibata, M.; Tanaka, A.; Maruya, K.; Onishi, T. *J. Chem. Soc., Chem. Commun.* **1986**, (23), 1706–1707.
(161) Sayama, K.; Tanaka, A.; Domen, K.; Maruya, K.; Onishi, T. *Catal. Lett.* **1990**, *4* (3), 217–222.
(162) Sayama, K.; Tanaka, A.; Domen, K.; Maruya, K.; Onishi, T. *J. Catal.* **1990**, *124* (2), 541–547.
(163) Tabata, S.; Ohnishi, H.; Yagasaki, E.; Ippommatsu, M.; Domen, K. *Catal. Lett.* **1994**, *28* (2–4), 417–422.
(164) Sayama, K.; Tanaka, A.; Domen, K.; Maruya, K.; Onishi, T. *J. Phys. Chem.* **1991**, *95* (3), 1345–1348.
(165) Yanagisawa, M.; Uchida, S.; Fujishiro, Y.; Sato, T. *J. Mater. Chem.* **1998**, *8* (12), 2835–2838.
(166) Furube, A.; Shiozawa, T.; Ishikawa, A.; Wada, A.; Domen, K.; Hirose, C. *J. Phys. Chem. B* **2002**, *106* (12), 3065–3072.
(167) Furube, A.; Shiozawa, T.; Ishikawa, A.; Wada, A.; Hirose, C.; Domen, K. *Chem. Phys.* **2002**, *285* (1), 31–37.
(168) Kim, Y. I.; Salim, S.; Huq, M. J.; Mallouk, T. E. *J. Am. Chem. Soc.* **1991**, *113* (25), 9561–9563.
(169) Domen, K.; Yoshimura, J.; Sekine, T.; Tanaka, A.; Onishi, T. *Catal. Lett.* **1990**, *4* (4–6), 339–343.
(170) Ebina, Y.; Sakai, N.; Sasaki, T. *J. Phys. Chem. B* **2005**, *109* (36), 17212–17216.

(171) Ebina, Y.; Tanaka, A.; Kondo, J. N.; Domen, K. *Chem. Mater.* **1996**, *8* (10), 2534–2538.
(172) Ebina, Y.; Sasaki, T.; Harada, M.; Watanabe, M. *Chem. Mater.* **2002**, *14* (10), 4390–4395.
(173) Compton, O. C.; Carroll, E. C.; Kim, J. Y.; Larsen, D. S.; Osterloh, F. E. *J. Phys. Chem. C* **2007**, *111* (40), 14589–14592.
(174) Yoshimura, J.; Ebina, Y.; Kondo, J.; Domen, K.; Tanaka, A. *J. Phys. Chem.* **1993**, *97* (9), 1970–1973.
(175) Kudo, A.; Hijii, S. *Chem. Lett.* **1999**, (10), 1103–1104.
(176) Zou, Z. G.; Ye, J. H.; Arakawa, H. *Chem. Mater.* **2001**, *13* (5), 1765–1769.
(177) Luan, J. F.; Zheng, S. R.; Hao, X. P.; Luan, G. Y.; Wu, X. S.; Zou, Z. G. *J. Braz. Chem. Soc.* **2006**, *17* (7), 1368–1376.
(178) Kudo, A.; Nakagawa, S.; Kato, H. *Chem. Lett.* **1999**, (11), 1197–1198.
(179) Hosogi, Y.; Tanabe, K.; Kato, H.; Kobayashi, H.; Kudo, A. *Chem. Lett.* **2004**, *33* (1), 28–29.
(180) Miseki, Y.; Kato, H.; Kudo, A. *Chem. Lett.* **2005**, *34* (1), 54–55.
(181) Miseki, Y.; Kato, H.; Kudo, A. *Chem. Lett.* **2006**, *35* (9), 1052–1053.
(182) Kudo, A.; Ueda, K.; Kato, H.; Mikami, I. *Catal. Lett.* **1998**, *53* (3–4), 229–230.
(183) Konta, R.; Kato, H.; Kobayashi, H.; Kudo, A. *Phys. Chem. Chem. Phys.* **2003**, *5* (14), 3061–3065.
(184) Kudo, A.; Kato, H. *Chem. Lett.* **1997**, (5), 421–422.
(185) Bamwenda, G. R.; Uesigi, T.; Abe, Y.; Sayama, K.; Arakawa, H. *Appl. Catal. A* **2001**, *205* (1–2), 117–128.
(186) Sayama, K.; Mukasa, K.; Abe, R.; Abe, Y.; Arakawa, H. *J. Photochem. Photobiol. A* **2002**, *148* (1–3), 71–77.
(187) Abe, R.; Takata, T.; Sugihara, H.; Domen, K. *Chem. Commun.* **2005**, (30), 3829–3831.
(188) Li, D. F.; Zheng, J.; Zou, Z. G. *J. Phys. Chem. Solids* **2006**, *67* (4), 801–806.
(189) Shimodaira, Y.; Kato, H.; Kobayashi, H.; Kudo, A. *J. Phys. Chem. B* **2006**, *110* (36), 17790–17797.
(190) Kudo, A.; Steinberg, M.; Bard, A. J.; Campion, A.; Fox, M. A.; Mallouk, T. E.; Webber, S. E.; White, J. M. *Catal. Lett.* **1990**, *5* (1), 61–66.
(191) Shimodaira, Y.; Kato, H.; Kobayashi, H.; Kudo, A. *J. Chem. Soc. Jpn.* **2007**, *80* (5), 885–893.
(192) Hara, M.; Kondo, T.; Komoda, M.; Ikeda, S.; Shinohara, K.; Tanaka, A.; Kondo, J. N.; Domen, K. *Chem. Commun.* **1998**, (3), 357–358.
(193) Ikeda, S.; Takata, T.; Kondo, T.; Hitoki, G.; Hara, M.; Kondo, J. N.; Domen, K.; Hosono, H.; Kawazoe, H.; Tanaka, A. *Chem. Commun.* **1998**, (20), 2185–2186.
(194) Wang, D. F.; Zou, Z. G.; Ye, J. H. *Chem. Mater.* **2005**, *17* (12), 3255–3261.
(195) Kimizuka, N.; Isobe, M.; Nakamura, M. *J. Solid State Chem.* **1995**, *116* (1), 170–178.
(196) Kudo, A.; Mikami, I. *Chem. Lett.* **1998**, (10), 1027–1028.
(197) Sato, J.; Saito, N.; Nishiyama, H.; Inoue, Y. *J. Phys. Chem. B* **2003**, *107* (31), 7965–7969.
(198) Wang, D. F.; Zou, Z. G.; Ye, J. H. *Chem. Phys. Lett.* **2004**, *384* (1–3), 139–143.
(199) Ikarashi, K.; Sato, J.; Kobayashi, H.; Saito, N.; Nishiyama, H.; Inoue, Y. *J. Phys. Chem. B* **2002**, *106* (35), 9048–9053.
(200) Sato, J.; Saito, N.; Nishiyama, H.; Inoue, Y. *J. Phys. Chem. B* **2001**, *105* (26), 6061–6063.
(201) Sato, J.; Saito, N.; Nishiyama, H.; Inoue, Y. *J. Photochem. Photobiol. A* **2002**, *148* (1–3), 85–89.
(202) Sato, J.; Kobayashi, H.; Ikarashi, K.; Saito, N.; Nishiyama, H.; Inoue, Y. *J. Phys. Chem. B* **2004**, *108* (14), 4369–4375.
(203) Maeda, K.; Takata, T.; Hara, M.; Saito, N.; Inoue, Y.; Kobayashi, H.; Domen, K. *J. Am. Chem. Soc.* **2005**, *127* (23), 8286–8287.
(204) Maeda, K.; Teramura, K.; Takata, T.; Hara, M.; Saito, N.; Toda, K.; Inoue, Y.; Kobayashi, H.; Domen, K. *J. Phys. Chem. B* **2005**, *109* (43), 20504–20510.
(205) Maeda, K.; Teramura, K.; Lu, D. L.; Saito, N.; Inoue, Y.; Domen, K. *Angew. Chem., Int. Ed.* **2006**, *45* (46), 7806–7809.
(206) Sato, J.; Saito, N.; Yamada, Y.; Maeda, K.; Takata, T.; Kondo, J. N.; Hara, M.; Kobayashi, H.; Domen, K.; Inoue, Y. *J. Am. Chem. Soc.* **2005**, *127* (12), 4150–4151.
(207) Maeda, K.; Saito, N.; Lu, D.; Inoue, Y.; Domen, K. Photocatalytic Properties of RuO_2-Loaded β-Ge_3N_4 for Overall Water Splitting. *J. Phys. Chem. C* **2007**, *111*, 4749–4755.
(208) Lee, Y.; Terashima, H.; Shimodaira, Y.; Teramura, K.; Hara, M.; Kobayashi, H.; Domen, K.; Yashima, M. *J. Phys. Chem. C* **2007**, *111* (2), 1042–1048.
(209) Hitoki, G.; Ishikawa, A.; Takata, T.; Kondo, J. N.; Hara, M.; Domen, K. *Chem. Lett.* **2002**, (7), 736–737.
(210) Hitoki, G.; Takata, T.; Kondo, J. N.; Hara, M.; Kobayashi, H.; Domen, K. *Chem. Commun.* **2002**, (16), 1698–1699.
(211) Hara, M.; Nunoshige, J.; Takata, T.; Kondo, J. N.; Domen, K. *Chem. Commun.* **2003**, (24), 3000–3001.
(212) Kasahara, A.; Nukumizu, K.; Hitoki, G.; Takata, T.; Kondo, J. N.; Hara, M.; Kobayashi, H.; Domen, K. *J. Phys. Chem. A* **2002**, *106* (29), 6750–6753.
(213) Liu, M. Y.; You, W. S.; Lei, Z. B.; Zhou, G. H.; Yang, J. J.; Wu, G. P.; Ma, G. J.; Luan, G. Y.; Takata, T.; Hara, M.; Domen, K.; Can, L. *Chem. Commun.* **2004**, (19), 2192–2193.
(214) Ohmori, T.; Mametsuka, H.; Suzuki, E. *Int. J. Hydrogen Energy* **2000**, *25* (10), 953–955.
(215) Evans, J. E.; Springer, K. W.; Zhang, J. Z. *J. Chem. Phys.* **1994**, *101* (7), 6222–6225.
(216) Gerische, H.; Meyer, E. *Z. Phys. Chem. Neue Folge* **1971**, *74* (3–6), 302-&.
(217) Reber, J. F.; Rusek, M. *J. Phys. Chem.* **1986**, *90* (5), 824–834.
(218) Darwent, J. R. *J. Chem. Soc., Faraday Trans. 2* **1981**, *77*, 1703–1709.
(219) Darwent, J. R.; Porter, G. *J. Chem. Soc., Chem. Commun.* **1981**, (4), 145–146.
(220) Buhler, N.; Meier, K.; Reber, J. F. *J. Phys. Chem.* **1984**, *88* (15), 3261–3268.
(221) Kalyanasundaram, K.; Borgarello, E.; Duonghong, D.; Gratzel, M. *Angew. Chem., Int. Ed. Engl.* **1981**, *20* (11), 987–988.
(222) Khan, M. M. T.; Bhardwaj, R. C.; Jadhav, C. M. *J. Chem. Soc., Chem. Commun.* **1985**, (23), 1690–1692.
(223) Tricot, Y. M.; Fendler, J. H. *J. Am. Chem. Soc.* **1984**, *106* (24), 7359–7366.
(224) Youn, H. C.; Baral, S.; Fendler, J. H. *J. Phys. Chem.* **1988**, *92* (22), 6320–6327.
(225) Hirai, T.; Shiojiri, S.; Komasawa, I. *J. Chem. Eng. Jpn.* **1994**, *27* (5), 590–597.
(226) Fujii, H.; Ohtaki, M.; Eguchi, K.; Arai, H. *J. Mol. Catal. A: Chem.* **1998**, *129* (1), 61–68.
(227) Sabate, J.; Cerveramarch, S.; Simarro, R.; Gimenez, J. *Int. J. Hydrogen Energy* **1990**, *15* (2), 115–124.
(228) Kakuta, N.; Park, K. H.; Finlayson, M. F.; Ueno, A.; Bard, A. J.; Campion, A.; Fox, M. A.; Webber, S. E.; White, J. M. *J. Phys. Chem.* **1985**, *89* (5), 732–734.
(229) Xing, C. J.; Zhang, Y. J.; Yan, W.; Guo, L. J. *Int. J. Hydrogen Energy* **2006**, *31* (14), 2018–2024.
(230) Kambe, S.; Fujii, M.; Kawai, T.; Kawai, S.; Nakahara, F. *Chem. Phys. Lett.* **1984**, *109* (1), 105–109.
(231) Sathish, M.; Viswanathan, B.; Viswanath, R. P. *Int. J. Hydrogen Energy* **2006**, *31* (7), 891–898.
(232) Rufus, I. B.; Viswanathan, B.; Ramakrishnan, V.; Kuriacose, J. C. *J. Photochem. Photobiol. A* **1995**, *91* (1), 63–66.
(233) Arai, T.; Sato, Y.; Shinoda, K.; Jeyadevan, B.; Tohji, K. Stratified Materials Synthesized in the Liquid Phase. In *Morphology Control of Materials and Nanoparticles*; Waseda, Y., Muramatsu, A., Eds.; Springer: Tokyo, 2003; Vol. 64, pp 65−84.
(234) Savinov, E. N.; Gruzdkov, Y. A.; Parmon, V. N. *Int. J. Hydrogen Energy* **1989**, *14* (1), 1–9.
(235) Borrell, L.; Cerveramarch, S.; Gimenez, J.; Simarro, R.; Andujar, J. M. *Sol. Energy Mater. Sol. Cells* **1992**, *25* (1–2), 25–39.
(236) Arora, M. K.; Sinha, A. S. K.; Upadhyay, S. N. *Ind. Eng. Chem. Res.* **1998**, *37* (10), 3950–3955.
(237) Jing, D. W.; Guo, L. J. *J. Phys. Chem. B* **2006**, *110* (23), 11139–11145.
(238) Yanagida, S.; Azuma, T.; Sakurai, H. *Chem. Lett.* **1982**, (7), 1069–1070.
(239) Kudo, A.; Sekizawa, M. *Catal. Lett.* **1999**, *58* (4), 241–243.
(240) Kudo, A.; Sekizawa, M. *Chem. Commun.* **2000**, (15), 1371–1372.
(241) Tsuji, I.; Kudo, A. *J. Photochem. Photobiol. A* **2003**, *156* (1–3), 249–252.
(242) Tsuji, I.; Kato, H.; Kudo, A. *Angew. Chem., Int. Ed.* **2005**, *44* (23), 3565–3568.
(243) Tsuji, I.; Kato, H.; Kudo, A. *Chem. Mater.* **2006**, *18* (7), 1969–1975.
(244) Kudo, A.; Tsuji, I.; Kato, H. *Chem. Commun.* **2002**, (17), 1958–1959.
(245) Tsuji, I.; Kato, H.; Kobayashi, H.; Kudo, A. *J. Am. Chem. Soc.* **2004**, *126* (41), 13406–13413.
(246) Zheng, N. F.; Bu, X. H.; Feng, P. Y. *J. Am. Chem. Soc.* **2005**, *127* (15), 5286–5287.
(247) Zheng, N.; Bu, X. H.; Vu, H.; Feng, P. Y. *Angew. Chem., Int. Ed.* **2005**, *44* (33), 5299–5303.
(248) Lei, Z. B.; Ma, G. J.; Liu, M. Y.; You, W. S.; Yan, H. J.; Wu, G. P.; Takata, T.; Hara, M.; Domen, K.; Li, C. *J. Catal.* **2006**, *237* (2), 322–329.
(249) Kobayakawa, K.; Teranishi, A.; Tsurumaki, T.; Sato, Y.; Fujishima, A. *Electrochim. Acta* **1992**, *37* (3), 465–467.
(250) Kudo, A.; Nagane, A.; Tsuji, I.; Kato, H. *Chem. Lett.* **2002**, (9), 882–883.
(251) Sobczynski, A.; Yildiz, A.; Bard, A. J.; Campion, A.; Fox, M. A.; Mallouk, T.; Webber, S. E.; White, J. M. *J. Phys. Chem.* **1988**, *92* (8), 2311–2315.
(252) Bessekhouad, Y.; Mohammedi, M.; Trari, M. *Sol. Energy Mater. Sol. Cells* **2002**, *73* (3), 339–350.
(253) Colombo, D. P.; Bowman, R. M. *J. Phys. Chem.* **1996**, *100* (47), 18445–18449.
(254) Jakob, M.; Levanon, H.; Kamat, P. V. *Nano Lett.* **2003**, *3* (3), 353–358.
(255) Sant, P. A.; Kamat, P. V. *Phys. Chem. Chem. Phys.* **2002**, *4* (2), 198–203.
(256) Wood, A.; Giersig, M.; Mulvaney, P. *J. Phys. Chem. B* **2001**, *105* (37), 8810–8815.
(257) Henglein, A.; Holzwarth, A.; Mulvaney, P. *J. Phys. Chem.* **1992**, *96* (22), 8700–8702.
(258) Serpone, N.; Lawless, D.; Khairutdinov, R. *J. Phys. Chem.* **1995**, *99* (45), 16646–16654.
(259) Inoue, Y.; Niiyama, T.; Asai, Y.; Sato, K. *J. Chem. Soc., Chem. Commun.* **1992**, (7), 579–580.
(260) Sato, J.; Saito, N.; Nishiyama, H.; Inoue, Y. *Chem. Lett.* **2001**, (9), 868–869.

CM7024203